

Two Puzzles, One Solution: Neutrino Mass and Secluded Dark Matter

Mattia Di Mauro^{1,*}

¹*Istituto Nazionale di Fisica Nucleare, Sezione di Torino, Via P. Giuria 1, 10125 Torino, Italy*

(Dated: November 26, 2025)

We present a minimal secluded dark-matter (DM) framework based on an extra $U(1)_X$ gauge symmetry. The model contains a Dirac DM particle χ , three heavy neutrinos N_I with masses $M_{N,I}$, and a singlet scalar R that mixes with the Standard Model Higgs doublet Φ by an angle α . A symmetry forbids the Φ - R portal at tree level; the leading portal then arises at one loop from the same Yukawa structures that generate active neutrino masses $m_{\nu,I}$, implying $\tan(2\alpha) \propto \sum_I m_{\nu,I} M_{N,I}^2 / (v_h m_H^2)$, where v_h and m_H are the SM Higgs VEV and mass. For heavy-neutrino masses in the multi-TeV range, this yields a naturally tiny mixing, $\tan(2\alpha) \sim 5 \times 10^{-11} (M_N/10 \text{ TeV})^2$, which strongly suppresses DM signals in direct, indirect, and collider searches. For PeV-scale heavy neutrinos the loop-induced portal is enhanced and the DM-nucleon cross section can instead enter the reach of direct-detection experiments. The visible and dark sectors thermalize at temperatures of order a few times the mass of the lightest heavy neutrino, then subsequently decouple, and typically evolve with a slightly hotter dark bath. In the secluded regime, with $\tan(2\alpha) \ll 1$ and $m_\chi > m_{H_p}$, the relic density is set by p -wave annihilation $\chi\bar{\chi} \rightarrow H_p H_p$ (with H_p the Higgs-like particle of the dark sector), and the dark-sector Yukawa couplings required to reproduce the observed abundance are $\mathcal{O}(0.1\text{--}1)$, as in the standard WIMP case. For heavy-neutrino masses $\gtrsim 10$ TeV, the mediator decays before nucleosynthesis without spoiling BBN observables, while the tiny portal suppresses present-day signals below current and near-future sensitivities. This links two long-standing puzzles – the absence of DM signals and the smallness of neutrino masses – within a predictive thermal framework.

Introduction. The existence of dark matter (DM) is firmly established through its gravitational effects, yet no laboratory experiment has detected any signal of DM–Standard Model (SM) interactions to date [1–3]. A viable DM candidate must be stable, neutral, non-relativistic at matter–radiation equality, and weakly interacting [3, 4]. WIMPs constitute a well-motivated class of DM candidates whose thermal freeze-out at electroweak scales naturally yields $\Omega_{\text{DM}} h^2 \simeq 0.12$ [5–10], motivating extensive direct, collider, and indirect searches [11–13] alongside cosmological observations [14].

Current limits, e.g., LZ and XENONnT, probe spin-independent cross sections down to $\mathcal{O}(10^{-47}\text{--}10^{-48}) \text{ cm}^2$ for weak-scale masses [15–17], excluding broad regions of parameter space for models where the same portal controls both freeze-out and scattering [18–22]. Resonant annihilation can evade these bounds, though typically at the price of mass tuning [20, 22]. A more generic alternative is *secluded* DM [23–25], in which the relic density is set by DM annihilating into mediator pairs within a dark sector while the SM portal (arising from Higgs mixing $\sin\alpha$ or gauge kinetic mixing) is parameterized by a coupling ϵ , which typically must satisfy $\epsilon \ll 10^{-3}$. Such a tiny portal might at first seem fine-tuned and theoretically unmotivated.

Interestingly, the SM already contains another unusu-

ally small mass scale: the active neutrino mass m_ν , with possible values in the tens-of-meV range [26–29], i.e., $\sim 10^{-7}$ of the electron mass.

We propose that the required smallness of the SM–dark portal is *not* fine-tuned but can be naturally connected to the small neutrino masses. In a minimal setup where a symmetry forbids the tree-level portal, the leading SM–dark coupling is generated radiatively by the same Yukawa structures that yield neutrino masses via a type-I seesaw [30–35]. The induced portal—either a Higgs mixing angle $\sin\alpha$ or a gauge kinetic mixing ϵ —then scales with m_ν up to loop factors and mass ratios. Consequently, direct, indirect, and collider signals are naturally suppressed—because m_ν is tiny—while the relic abundance remains set by DM annihilations into dark mediator pairs and is largely decoupled from the portal.

Model Lagrangian and particle content. We consider a minimal BSM dark-sector setup that is UV-complete and can realize the secluded DM mechanism. We introduce an extra abelian gauge group $U(1)_X$ containing a Dirac fermion χ with charge q_X^χ , singlet under the SM gauge groups, a massive gauge boson Z' with coupling g_X , three right-handed neutrinos N_i ($i = 1, 2, 3$), and a complex scalar singlet R that mixes with the SM Higgs doublet Φ (see e.g. [36, 37]). We report all the details in App. A and summarize here its main features. The relevant Lagrangian terms are

$$\mathcal{L} \supset -\frac{1}{4} F'_{\mu\nu} F'^{\mu\nu} - \frac{\epsilon}{2} F'_{\mu\nu} B^{\mu\nu} + \partial_\mu R^\dagger \partial^\mu R - V(\Phi, R) + \bar{\chi} (i \not{D} - m_\chi) \chi - \left(y_p \bar{\chi} \chi R + Y_\nu^{\alpha i} \bar{L}_\alpha \tilde{\Phi} N_i + \frac{1}{2} Y_N^{ij} R \bar{N}_i^c N_j + \text{h.c.} \right), \quad (1)$$

* dimauro.mattia@gmail.com

where $L_\alpha = (\nu_{\alpha L}, \ell_{\alpha L})^T$ are the SM lepton doublets, Φ is the SM Higgs, $B_{\mu\nu}$ is the hypercharge field-strength tensor, Y_ν and $Y_N = Y_N^T$ are the generic complex 3×3 Yukawa matrices coupling Φ and R to the light and heavy neutrinos. We take χ to be vector-like under $U(1)_X$, i.e., $q_L^\chi = q_R^\chi = q_X^\chi$. Then a bare Dirac mass term $m_0 \bar{\chi}\chi$ is gauge invariant if R is neutral ($q_X^R = 0$), and we can add a renormalizable Yukawa portal $-y_p \bar{\chi}\chi R$. In this case $U(1)_X$ is not broken by R acquiring a vacuum expectation value (VEV) $v_r = \langle R \rangle$, and the Z' mass can be generated via a Stückelberg mechanism. Since χ is vector-like, y_p is not fixed by m_χ ($m_\chi = m_0 + y_p v_r / \sqrt{2}$). Here $F'_{\mu\nu}$, g_X , and $m_{Z'}$ denote the field strength, coupling, and mass of the new gauge boson Z'_μ . The term $-\frac{\epsilon}{2} F'_{\mu\nu} B^{\mu\nu}$ represents kinetic mixing between $U(1)_X$ and hypercharge, controlled by ϵ [38, 39]. In the following we neglect this mixing (or assume it is sufficiently small). SM fermions are neutral under $U(1)_X$, so they do not couple directly to Z' at tree level.

The (R, Φ) scalar potential is

$$V(\Phi, R) = \mu_H^2 \Phi^\dagger \Phi + \mu_R^2 R^\dagger R + \lambda_H (\Phi^\dagger \Phi)^2 + \lambda_R (R^\dagger R)^2 + \kappa (\Phi^\dagger \Phi)(R^\dagger R). \quad (2)$$

After electroweak symmetry breaking (EWSB) $\Phi \rightarrow (v_h + h)/\sqrt{2}$ and $R \rightarrow (v_r + \rho)/\sqrt{2}$, the CP-even mass matrix in the (h, ρ) basis is

$$\mathcal{M}^2 = \begin{pmatrix} 2\lambda_H v_h^2 & \kappa v_h v_r \\ \kappa v_h v_r & 2\lambda_R v_r^2 \end{pmatrix}, \quad \tan 2\alpha = \frac{\kappa v_h v_r}{\lambda_R v_r^2 - \lambda_H v_h^2}, \quad (3)$$

which is diagonalized by a rotation of angle α , yielding the SM-like state H and the singlet-like state H_p with masses m_H and m_{H_p} .

Type-I seesaw. We summarize the main aspects of light and heavy neutrino masses, couplings, and the seesaw mechanism; a more detailed discussion is given in App. B. Taking the heavy Majorana mass matrix to be $M_N = \frac{v_r}{\sqrt{2}} Y_N$ and the Dirac mass matrix $m_D = \frac{v_h}{\sqrt{2}} Y_\nu$, the Majorana-like neutrino mass matrix in the (ν_L, N^c) basis is

$$\mathcal{M}_\nu = \begin{pmatrix} 0 & m_D \\ m_D^T & M_N \end{pmatrix}. \quad (4)$$

For $\|m_D\| \ll \|M_N\|$ one obtains the standard type-I seesaw relation

$$M_\nu \simeq -m_D M_N^{-1} m_D^T. \quad (5)$$

Since Y_N is symmetric, M_N is diagonalized by a Takagi factorization, defining the heavy-Majorana-neutrino mass eigenstates N_I with masses $M_{N,I} > 0$ ($I = 1, 2, 3$) and diagonal Yukawa entries $y_{N,I} = \sqrt{2} M_{N,I} / v_r$. The light-neutrino mass matrix M_ν is diagonalized by the PMNS matrix U_ν , yielding the physical light eigenstates ν_i with masses m_i . The Majorana mass term breaks the global lepton number symmetry $U(1)_L$ by two units ($\Delta L = 2$), so the light neutrinos are Majorana.

In this letter we work in the basis where the heavy-neutrino Majorana mass matrix is diagonal, and we parameterize the Dirac mass matrix via the Casas-Ibarra form [40]:

$$m_D = i U_\nu \sqrt{\hat{m}_\nu} O \sqrt{\hat{M}_N}, \quad (6)$$

where $\hat{m}_\nu = \text{diag}(m_{\nu,1}, m_{\nu,2}, m_{\nu,3})$ and O is a complex orthogonal matrix, $O^T O = \mathbb{1}$. In the *aligned limit* we take $O = \mathbb{1}$ and use the freedom to label the heavy eigenstates so that each heavy mass $M_{N,I}$ is paired with the corresponding light eigenvalue $m_{\nu,I}$. In this case,

$$(Y_\nu^\dagger Y_\nu)_{II} = \sum_{\alpha=e,\mu,\tau} |y_{\alpha I}|^2 = \frac{2 m_{\nu,I} M_{N,I}}{v_h^2}. \quad (7)$$

The usual effective seesaw mass parameter for N_I becomes $m_{\nu,I}$,

$$\tilde{m}_I \equiv \frac{(m_D^\dagger m_D)_{II}}{M_{N,I}} = m_{\nu,I} = \frac{v_h^2}{2} \frac{|y_{\nu,I}|^2}{M_{N,I}}. \quad (8)$$

where $y_{\nu,I}$ are the Yukawa couplings associated to $m_{\nu,I}$ as defined in Eq. 7.

WIMP and secluded regimes. The WIMP regime applies for $m_\chi < m_{H_p}$ with $y_p \sim \mathcal{O}(1)$ and $\sin \alpha \sim \mathcal{O}(0.1)$. In this case, the dominant annihilation channels are $\chi \bar{\chi} \rightarrow f \bar{f}$ through s -channel exchange of H or H_p , with

$$\langle \sigma v \rangle_{f \bar{f}} \propto y_p^2 (\sin \alpha \cos \alpha)^2. \quad (9)$$

In this regime DM can reach the correct relic density for $y_p \sim 0.1$ –1, but these couplings are almost entirely ruled out by direct-detection limits (except near the resonance $m_\chi \simeq m_{H_p}/2$), see Ref. [25].

In the secluded case, valid for $m_\chi > m_{H_p}$ with $y_p \sim \mathcal{O}(0.1)$ and $\sin \alpha \ll 1$, annihilations into dark-sector states dominate, e.g. $\chi \bar{\chi} \rightarrow H_p H_p$, with

$$\langle \sigma v \rangle_{H_p H_p} \propto \frac{v_{\text{rel}}^2 y_p^4}{m_\chi^2}, \quad (10)$$

where v_{rel} is the DM relative velocity. Spin-independent scattering on nucleons proceeds via t -channel H or H_p exchange and scales as

$$\sigma_{\chi N}^{\text{SI}} \propto y_p^2 \cos^2 \alpha \sin^2 \alpha \propto y_p^2 (\tan 2\alpha)^2, \quad (11)$$

so in the secluded regime the nuclear cross section and indirect detection (see Eq. 9) are highly suppressed ($\tan 2\alpha \ll 1$), while for $y_p \sim \mathcal{O}(0.1$ –1) the process $\chi \bar{\chi} \rightarrow H_p H_p$ yields $\Omega_{\text{DM}} h^2 \simeq 0.12$. Throughout, since we work in the secluded case, we use $\tan 2\alpha$ to characterize the mixing strength between Φ and R .

Tree-level portals set to zero. The scalar portal $|R|^2 |\Phi|^2$ (a similar reasoning can be applied to the abelian kinetic mixing $\epsilon F_Y^{\mu\nu} F_{\mu\nu}^D$) is gauge-invariant and thus generic in 4D renormalizable EFTs [38, 41]. We therefore impose

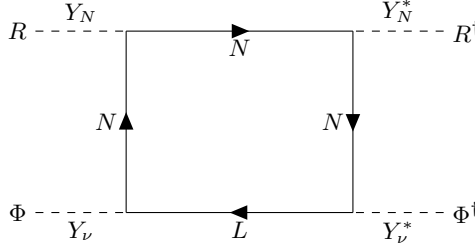


FIG. 1. Box Feynman diagram describing the one-loop generation of the mixed quartic $(R^\dagger R)(\Phi^\dagger \Phi)$.

$\kappa(\Lambda) = 0$ at the UV scale (Λ), and arrange that the only fields communicating between the SM and the dark sector are the neutrino-sector spurions (the mass matrix M_N) that also generate the light neutrino masses $m_{\nu,I}$. This makes any nonzero portal *radiative* and aligned with neutrino-mass breaking. If $\kappa(\Lambda) = 0$ at tree level, the running of the portal at lower energies also remains zero. This is due to the fact that the function $\beta_\kappa = dk/d\log\mu$ does not have any additive terms (see App. F).

Two standard UV mechanisms that ensure a vanishing tree-level portal are technically natural: (i) **Sequestering of sectors.** In extra-dimensional or sequestered SUSY setups the renormalizable Lagrangian factorizes, so $|H|^2|\Phi|^2$ is absent at tree level and is induced only by messengers in the loops (here, the N_i) [42–45]. (ii) **Gauge-portal protection.** For kinetic mixing, either a non-abelian UV origin $G_D \supset U(1)_D$ forbids $F_Y F_D$ until symmetry breaking [38, 41], or a dark charge-conjugation C_D makes $F_Y F_D$ odd, so ϵ first appears with the same spurions that generate m_ν [24, 46].

Loop-induced portal from the neutrino sector. At one loop an effective vertex $\kappa_{\text{loop}}(\Phi^\dagger \Phi)(R^\dagger R)$ arises from a box diagram with two ΦLN and two $R NN$ insertions (see Fig. 1). Considering three heavy singlets N_I and working in the aligned Casas–Ibarra limit for the Dirac mass matrix, in dimensional regularization (MS) and matching at the renormalization scale $\mu = M_N$, the loop-induced coupling is

$$\kappa_{\text{loop}} = - \sum_{I=1}^3 \frac{y_{N,I}^2 M_{N,I}}{8\pi^2 v_h^2} m_{\nu,I}, \quad (12)$$

which makes explicit the parametric correlation with the light neutrino masses $\kappa_{\text{loop}} \propto \sum_I m_{\nu,I}$. For momenta

$|p^2| \ll M_{N,I}^2$, the one-loop amplitude matches onto the local operator $(\Phi^\dagger \Phi)(R^\dagger R)$, so we use κ_{loop} as the effective $\Phi\Phi RR$ contact coupling that is valid for freeze-out, direct detection, and the collider observables.

Relation between the mixing angle and m_ν . At tree level the scalar mixing angle α between the SM-like Higgs H and the singlet-like state H_p is controlled by the portal coupling κ via Eq. (3). Using Eq. (3) with $\kappa = \kappa_{\text{loop}}$ from Eq. (12) and $M_N = y_N v_r / \sqrt{2}$, one finds for a single generation

$$\begin{aligned} \tan 2\alpha &= - \frac{|m_\nu| y_N M_N^2}{2\sqrt{2} \pi^2 v_h (m_{H_p}^2 - m_H^2)} \\ &\simeq - \frac{4.66 \times 10^{-11}}{1 - (m_{H_p}/125 \text{ GeV})^2} y_N \left(\frac{|m_\nu|}{0.05 \text{ eV}} \right) \left(\frac{M_N}{10 \text{ TeV}} \right)^2. \end{aligned} \quad (13)$$

For three generations (e.g. in the Casas–Ibarra aligned limit) the result generalizes by $y_N M_N^2 |m_\nu| \rightarrow \sum_I y_{N,I} M_{N,I}^2 |m_{\nu,I}|$.

Therefore, the H – H_p mixing that controls the SM–dark sector portal is directly proportional to the light neutrino masses. The smallness of m_ν (from the seesaw mechanism) explains the small portal. In particular, values $\tan 2\alpha \sim 10^{-11}$ render direct, indirect, and collider signals essentially undetectable with current and next-generation experiments (see [25]).

Dark matter relic density. Here we detail how DM attains the observed relic density, following the evolution of the SM and hidden sectors from very high temperatures, when the heavy neutrinos are ultra-relativistic ($T \gg M_N$), down to the BBN epoch at $t_{\text{BBN}} \sim 1$ s.

We start from the end, i.e. the BBN epoch. We focus on the secluded regime with $m_\chi > m_{H_p}$ and $\tan(2\alpha) \ll 1$, so that $\chi\chi \rightarrow H_p H_p$ controls the relic abundance. After DM freezes out in the hidden sector, the produced H_p remains in the dark bath and subsequently decays into SM fermions; if these decays occur after BBN, they can spoil light-element abundances.

Neglecting threshold effects and summing over open fermionic channels for $m_{H_p} \in [20, 100]$ GeV, a convenient parametrization of the H_p lifetime is

$$\tau_{\text{ferm}}(H_p) = \frac{1}{\Gamma_{\text{ferm}}} \approx 4.3 \times 10^{-21} \text{ s} \left(\frac{20 \text{ GeV}}{m_{H_p}} \right) \frac{1}{(\tan 2\alpha)^2}, \quad (14)$$

up to $\mathcal{O}(1)$ factors from channel thresholds. Using the loop-induced mixing and $\tan 2\alpha$ relation of Eq. (14) one obtains for one generation

$$\tau_{\text{ferm}}(H_p) \simeq \left(\frac{1.20 \text{ s}}{y_N^2} \right) \left(\frac{20 \text{ GeV}}{m_{H_p}} \right) \left(\frac{16 \text{ TeV}}{M_N} \right)^4 \left(\frac{0.05 \text{ eV}}{m_\nu} \right)^2 \left[1 - \left(\frac{m_{H_p}}{125 \text{ GeV}} \right)^2 \right]^2. \quad (15)$$

Figure 2 confirms this scaling by showing the (m_{H_p}, M_N) region where $H_p \rightarrow f\bar{f}$ occurs before BBN

$(\tau_{\text{ferm}} < \tau_{\text{BBN}})$, assuming $y_N = 1$ and $m_\nu = 0.05$ eV. For $m_{H_p} \lesssim 100$ GeV, larger m_{H_p} requires smaller M_N to keep

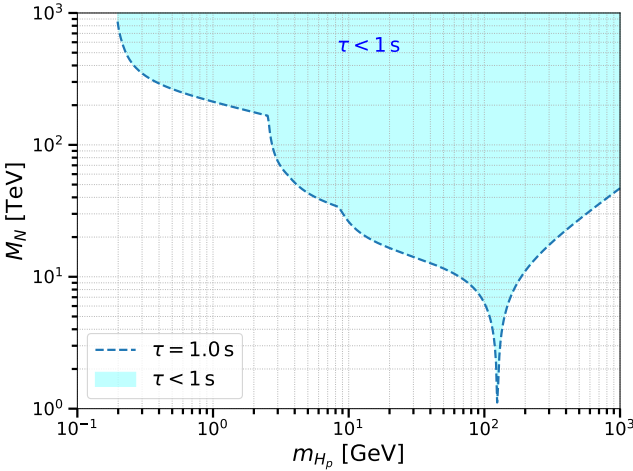


FIG. 2. Values of the heavy-neutrino mass M_N and dark scalar mass m_{H_p} for which the decay of H_p occurs before BBN. We fix $y_N = 1$ and $m_\nu = 0.05$ eV.

$\tau_{\text{ferm}} < 1$ s. A pronounced dip appears as $m_{H_p} \rightarrow m_H$; for $m_{H_p} > m_H$, the trend reverses and the allowed M_N increase roughly with m_{H_p} . Away from the resonance, one typically needs $M_N \gtrsim 10$ TeV to ensure $\tau_{\text{ferm}} < 1$ s.

Since we work with WIMP-range m_χ and require $m_\chi > m_{H_p}$ (secluded regime), and because BBN safety favors $M_N \gtrsim 10$ TeV to guarantee prompt H_p decays into SM fermions, in what follows we assume the mass hierarchy

$$M_N > m_\chi > m_{H_p}. \quad (16)$$

When several heavy Majorana eigenstates N_I are present, the slowest (last) to lose equilibrium is the *lightest* one. It is therefore sufficient (and conservative) to track a single state N with mass $M_N \equiv \min_I(M_{N,I})$. In the aligned limit, we denote by m_ν the light eigenvalue paired with this lightest N .

Era I ($T \gg M_N$). For temperatures above the heavy-neutrino threshold, the SM and the hidden sector are connected by the neutrino portal. The relevant processes are: (i) decays/inverse decays $N \leftrightarrow L_\alpha H, \bar{L}_\alpha H^\dagger$; (ii) $\Delta L = 1$ scatterings with one neutrino Yukawa and one SM coupling, such as $N L_\alpha \leftrightarrow Q_{3t}$ (top-assisted) and $L_\alpha A \leftrightarrow NH$ (gauge-assisted), with A an electroweak gauge boson; (iii) $\Delta L = 2$ scatterings $LH \leftrightarrow \bar{L}H^\dagger, LL \leftrightarrow HH$ induced by virtual N ; and (iv) portal reactions involving the dark scalar R and χ , including $NR \leftrightarrow L_\alpha H$ and $RR \leftrightarrow HH$. A complete discussion is given in App. D.

For the lightest state N (mass M_N), the thermally averaged rate for the decay into LH and $\bar{L}H^\dagger$ in the unbroken phase and aligned limit is

$$\langle \Gamma_D \rangle_T = \Gamma_D \frac{K_1(\xi)}{K_2(\xi)}, \quad \Gamma_D = \frac{m_\nu M_N^2}{4\pi v_h^2}, \quad (17)$$

with $\xi \equiv M_N/T$. $\langle \Gamma_D \rangle_T$ should be compared with $H(T) = 1.66\sqrt{g_*} T^2/M_{\text{Pl}}$. Solving $\langle \Gamma_D \rangle_T = H(T)$ in

the relativistic regime gives

$$\frac{T_*}{M_N} \simeq \left[\frac{m_\nu M_{\text{Pl}}}{13.28\pi\sqrt{g_*} v_h^2} \right]^{1/3} \simeq 2.8 \left(\frac{m_\nu}{0.05 \text{ eV}} \right)^{1/3} \left(\frac{106.75}{g_*} \right)^{1/6}, \quad (18)$$

so N is in thermal equilibrium with the SM bath for $T \gtrsim \text{few} \times M_N$. At $T = M_N$ one finds

$$\left. \frac{\langle \Gamma_D \rangle_T}{H} \right|_{T=M_N} \sim \mathcal{O}(20-30) \quad \text{for } m_\nu \sim 0.05 \text{ eV}, \quad (19)$$

showing that decays/inverse decays alone efficiently maintain contact near and above $T \sim M_N$ for seesaw-motivated parameters.

The leading $\Delta L = 1$ scatterings provide an additional contribution. Summing the dominant top- and gauge-assisted channels one finds

$$\frac{\Gamma_{\text{scatt}}^{(\Delta L=1)}(T)}{H(T)} \simeq \frac{2c_1}{1.66\sqrt{g_*}} \frac{m_\nu M_{\text{Pl}}}{v_h^2} (y_t^2 + g^2) \frac{M_N}{T} \sim \mathcal{O}(1) \frac{M_N}{T}, \quad (20)$$

where $c_1 \simeq (3-7) \times 10^{-4}$ and y_t is the top quark Yukawa. Thus $\Delta L = 1$ scattering rates are of the same order as H around $T \sim M_N$ (and subleading at $T \gg M_N$), reinforcing equilibration that is dominated by decays/inverse decays. The $\Delta L = 2$ scatterings become efficient only at very high temperatures $T \gtrsim 10^{12}$ GeV and are negligible in the range relevant here.

Among the portal processes, the loop-induced $RR \leftrightarrow HH$ is negligible for our parameters, while $NR \leftrightarrow L_\alpha H$, controlled by y_N and y_ν , for $y_N = \mathcal{O}(1)$ satisfies $\Gamma/H \sim 0.1-0.2$ near $T \sim M_N$. In this regime, together with N decays/inverse decays and the $\Delta L = 1$ scatterings, the $NR \leftrightarrow L_\alpha H$ channel efficiently transfers energy between the visible and dark sectors, so that once N is thermalized the dark scalar and χ are also brought into equilibrium.

Overall, in Era I the neutrino portal is very efficient: decays/inverse decays of N , $\Delta L = 1$ scatterings, and (when present with sizeable y_N) the $NR \leftrightarrow LH$ channel guarantee thermal contact between the SM and the dark sector.

In Fig. 3 we compare the relevant per-particle rates to $H(T)$ ¹ as a function of ξ for the benchmark $M_N = 20$ TeV, $m_\nu = 0.05$ eV, and $y_N = 1$. The thermally averaged decay/inverse-decay rate $\langle \Gamma_D \rangle$ exceeds $H(T)$ around and above $T \sim M_N$, ensuring efficient equilibration between N and the SM bath. The $\Delta L = 1$ scatterings, shown as a band from the uncertainty in c_1 , contribute at the level of H near $T \sim M_N$ and remain comparable to H for $T \gtrsim M_N$, reinforcing thermal contact. The portal scattering $NR \leftrightarrow L_\alpha H$ is also efficient for the chosen parameters ($y_N = \mathcal{O}(1)$), with $\Gamma/H \sim \mathcal{O}(0.1-1)$

¹ The figure shows *per-particle* rates Γ , which by construction do not exhibit Boltzmann suppression for $T \lesssim M_N$. That suppression enters instead through the *reaction density* $\gamma(T) \equiv n_N^{\text{eq}}(T) \langle \Gamma \rangle$, with $n_N^{\text{eq}}(T) \propto (M_N T)^{3/2} e^{-M_N/T}$.

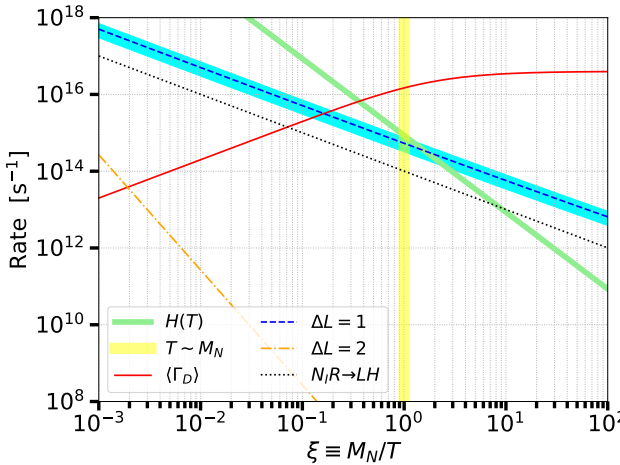


FIG. 3. Per-particle rates vs. expansion rate for the neutrino-portal processes as a function of $\xi = M_N/T$: decay/inverse decay $N \leftrightarrow LH$ (red solid), $\Delta L = 1$ scatterings (blue dashed), $NR \leftrightarrow L_\alpha H$ (black dotted), and $\Delta L = 2$ scatterings (orange dot-dashed). We fix $M_N = 20$ TeV, $m_\nu = 0.05$ eV, and $y_N = 1$. The green band shows $H(T)$; the cyan band reflects the uncertainty on the coefficient c_1 in the $\Delta L = 1$ rate. The vertical yellow band marks the transition to the non-relativistic regime for N where its abundance becomes Boltzmann suppressed.

throughout the range where N is still abundant; once N is in equilibrium, the dark scalar and χ are therefore brought into equilibrium with the SM as well. In contrast, the $\Delta L = 2$ rates remain well below $H(T)$ at these scales and do not affect equilibration. For $T \lesssim M_N$ ($\xi \gtrsim 1$), the number density of N becomes Boltzmann suppressed; all N -mediated processes effectively decouple, and the neutrino portal ceases to maintain thermal contact.

Era II (decoupling around $T \sim M_N$). As T drops below the (lightest) heavy-neutrino mass, the N abundance becomes Boltzmann suppressed and inter-sector energy exchange shuts off at temperature $T_{\text{dec}} \sim (0.2 - 0.3)M_N$. After visible-dark decoupling, the *comoving entropies* of the two sectors are separately conserved. Assuming the dark sector was in full chemical equilibrium at decoupling ($\mu_i(T'_{\text{dec}}) = 0$, where μ_i is the chemical potential for the particle i) and that, thereafter, both sectors remain effectively ultrarelativistic with vanishing chemical potentials ($s = \frac{2\pi^2}{45} g_{*S} T^3$), the temperature ratio is [47]

$$\zeta = \frac{T'}{T} = \left[\frac{g_{*S}^{\text{vis}}(T)}{g_{*S}^{\text{vis}}(T_{\text{dec}})} \right]^{1/3} \left[\frac{g_{*S}^{\text{dark}}(T'_{\text{dec}})}{g_{*S}^{\text{dark}}(T')} \right]^{1/3}. \quad (21)$$

This holds only while both baths are relativistic with $\mu_i = 0$; if any species becomes non-relativistic or $\mu_i \neq 0$, one must use the general entropy-conservation expression (see App. G). Whether $\zeta = T'/T$ exceeds unity depends on the relative entropy dumps after decoupling: $\zeta > 1$ if the visible sector loses more relativistic degrees of freedom than the dark sector (and vice versa). For GeV-scale

DM and multi-TeV heavy neutrinos one typically finds $\zeta \simeq 1-2$.

*Era III (DM freeze-out in a hotter dark bath).*² For $m_\chi > m_{H_p}$ (secluded regime), $\chi\chi \rightarrow H_p H_p$ keeps the dark bath thermal at $T' = \zeta T$, while the portal is far too small to re-equilibrate with the SM. Working with $x \equiv m_\chi/T$ and $x' = x/\zeta$, the Boltzmann equation for the comoving yield $Y_\chi \equiv n_\chi/s_{\text{vis}}$ (defined with the *visible* entropy density) reads

$$\frac{dY_\chi}{dx} = -\frac{s_{\text{vis}}(T)}{x H(T)} \langle \sigma v \rangle_{\chi\chi \rightarrow H_p H_p}(T') \left[Y_\chi^2 - (Y_\chi^{\text{eq}}(T'))^2 \right], \quad (22)$$

with $Y_\chi^{\text{eq}}(T') = n_\chi^{\text{eq}}(T')/s_{\text{vis}}(T) \propto x'^2 K_2(x')$ the *dark* equilibrium abundance. During radiation domination the Hubble rate depends on the *total* relativistic energy density from both sectors,

$$H(T) = \frac{\pi}{\sqrt{90}} \frac{T^2}{M_{\text{Pl}}} \left[g_*^{\text{vis}}(T) + g_*^{\text{dark}}(T') \zeta^4 \right]^{1/2},$$

where $g_*^{\text{vis}}(T)$ and $g_*^{\text{dark}}(T')$ are the usual *energy* degrees of freedom, and we define $g_*^H(T, T') = g_*^{\text{vis}}(T) + \zeta^4 g_*^{\text{dark}}(T')$.

The freeze-out condition is $n_\chi^{\text{eq}}(T') \langle \sigma v \rangle(T') \simeq H(T)$ and we can use the following iterative solution to find the freeze-out temperature, which for m_χ at the GeV-TeV scale and $y_p \sim \mathcal{O}(0.1-1)$ is $x'_f \in [20, 30]$, as in the standard WIMP case. The relic density then follows from the asymptotic yield $Y_{\chi, \infty} \equiv Y_\chi(T \rightarrow 0)$,

$$\Omega_\chi h^2 \simeq \left(1.05 \times 10^9 \text{ GeV}^{-1} \right) \frac{\sqrt{g_*^H(T_f, T'_f)} \zeta x'^2_f}{g_*^{\text{vis}}(T_f) M_{\text{Pl}}} \frac{64\pi m_\chi^2}{3 y_p^4}. \quad (23)$$

Inverting Eq. (23) yields the coupling required to reproduce the observed abundance, which is of order $\mathcal{O}(0.1 - 1)$,

$$y_p \simeq 0.43 \left(\frac{x'_f}{25} \right)^{1/2} \left(\frac{m_\chi}{100 \text{ GeV}} \right)^{1/2} \left(\frac{g_{*S}^{\text{vis}}}{86.25} \right)^{-1/4} \left(\frac{g_*^H}{100} \right)^{1/8}. \quad (24)$$

A convenient estimate for the required thermal cross section is $\langle \sigma v \rangle \approx 2 \times 10^{-26} \text{ cm}^3 \text{s}^{-1}/\zeta$ i.e. a *hotter* bath ($\zeta > 1$) requires a smaller $\langle \sigma v \rangle$ with respect to the canonical WIMP thermal cross section [47].

Nuclear cross-section upper limits The upper limits from LZ [17] on the spin-independent nuclear cross section σ_{LZ} provide the following constraint on the parameter space for $m_\chi = 100$ GeV (see App. H for the full calculation and the results given as a function of m_χ)

$$\begin{aligned} \sigma_{\chi N}^{\text{SI}} &\simeq 3.9 \times 10^{-57} \text{ cm}^2 \left(\frac{y_p}{1} \right)^2 \left(\frac{10 \text{ GeV}}{m_{H_p}} \right)^4 \times \\ &\times \sum_{I=1}^3 \left(\frac{y_{N,I}}{1} \right)^2 \left(\frac{m_{\nu,I}}{0.05 \text{ eV}} \right)^2 \left(\frac{M_{N,I}}{10 \text{ TeV}} \right)^4 \lesssim \sigma_{\text{LZ}}. \end{aligned} \quad (25)$$

² See App. G for the full details of the calculations reported here.

Fixing y_p to the value that provides the correct relic density (see Eq. 24) and taking $y_N \sim 1$, Eq. 25 can be translated into an upper limit on the heavy neutrino mass. For $m_{H_p} = 10$ GeV and one generation one finds

$$M_N \lesssim 1.7 \times 10^3 \text{ TeV} \left(\frac{1}{y_p y_N} \right)^{1/2} \left(\frac{0.05 \text{ eV}}{m_\nu} \right)^{1/2} \left(\frac{m_{H_p}}{10 \text{ GeV}} \right). \quad (26)$$

Conclusions We introduced a minimal secluded-DM setup embedded in an extra $U(1)_X$ with a Dirac dark fermion χ and a Higgs-like singlet R , where the Higgs-singlet portal vanishes at tree level and is *radiatively* generated by the neutrino sector. The loop-induced R - Φ mixing obeys $\tan(2\alpha) \sim \sum_I 5 \times 10^{-11} \left(\frac{m_{\nu,I}}{0.05 \text{ eV}} \right) \left(\frac{M_{N,I}}{10 \text{ TeV}} \right)^2$ linking the portal directly to the light-neutrino masses $m_{\nu,I}$ and to the heavy singlets N_I (with masses $M_{N,I}$). In short, the non-observation of WIMP-like signals can be connected to the smallness of SM active neutrino masses: the tiny m_ν makes the portal naturally minuscule, strongly suppressing direct, indirect, and collider signals today, turning the lack of detection into an *natural expectation*. In particular, for heavy-neutrino masses $\gtrsim 10$ TeV, the loop-induced spin-independent nuclear cross section remains far below the sensitivity of current and foreseeable direct-detection experiments, rendering this scenario effectively invisible in standard nuclear-recoil searches. Instead, for PeV-

scale heavy neutrinos the loop-induced portal is enhanced and the DM–nucleon cross section can enter the reach of direct-detection experiments. Moreover, for even larger masses $M_{N,I} \gtrsim 10^3$ TeV the model naturally enters the parametric regime of standard thermal or resonant leptogenesis, so that the out-of-equilibrium, CP-violating decays of N_I can also account for the observed matter–antimatter asymmetry of the Universe [48–50]. In the secluded regime, with $\tan(2\alpha) \ll 1$ and $m_\chi > m_{H_p}$, the relic density is set by p -wave annihilation $\chi\bar{\chi} \rightarrow H_p H_p$, and the dark-sector Yukawa couplings required to reproduce the observed abundance are $\mathcal{O}(0.1\text{--}1)$, as in the standard WIMP case.

ACKNOWLEDGMENTS

M.D.M. thanks N.Fornengo, S.Gariazzo for reading the paper and providing us very helpful comments and suggestions. M.D.M. acknowledges support from the research grant *TAsP (Theoretical Astroparticle Physics)* funded by Istituto Nazionale di Fisica Nucleare (INFN) and from the Italian Ministry of University and Research (MUR), PRIN 2022 “EXSKALIBUR – Euclid-Cross-SKA: Likelihood Inference Building for Universe’s Research”, Grant No. 20222BBYB9, CUP I53D23000610 0006, and from the European Union – Next Generation EU.

Appendix A: General Details of the Model

In this appendix we provide the full model details. Section A 1 presents the Lagrangian, particle content, and the most relevant couplings. In Sec. A 2 we describe the Φ – R scalar mixing. In Sec. A 3 we collect the interaction terms in the mass basis. In Sec. A 4 we list useful decay rates and annihilation cross sections.

1. Lagrangian and Particle Content

We consider a minimal UV–complete BSM dark sector that realizes the secluded mechanism [23–25]. The model features an extra abelian gauge group $U(1)_X$ containing a Dirac fermion χ with charge q_X^χ (singlet under the SM gauge groups), a massive gauge boson Z' with coupling g_X , three right-handed neutrinos N_i ($i = 1, \dots, 3$), and a complex scalar singlet R that mixes with the SM Higgs doublet Φ (see e.g. [36, 37]). The relevant Lagrangian terms are given by

$$\begin{aligned} \mathcal{L} \supset & -\frac{1}{4}F'_{\mu\nu}F'^{\mu\nu} - \frac{\epsilon}{2}F'_{\mu\nu}B^{\mu\nu} + \partial_\mu R^\dagger \partial^\mu R - V(\Phi, R) + \bar{\chi}(iD - m_\chi)\chi \\ & - \left(y_p \bar{\chi}\chi R + \text{h.c.}\right) - \left(Y_\nu^{\alpha i} \bar{L}_\alpha \tilde{\Phi} N_i + \frac{1}{2}Y_N^{ij} R \bar{N}_i^c N_j + \text{h.c.}\right), \end{aligned} \quad (\text{A1})$$

where $L_\alpha = (\nu_{\alpha L}, \ell_{\alpha L})^T$ are the SM lepton doublets, Φ is the SM Higgs, $B_{\mu\nu}$ is the hypercharge field–strength tensor, and Y_ν (3×3 complex) and $Y_N = Y_N^T$ (complex symmetric) are the neutrino Yukawa matrices.

In what follows we take χ to be vector-like, $q_{\chi_L} = q_{\chi_R} = q_\chi$. Then a bare mass $m_0 \bar{\chi}\chi$ is gauge invariant if R is neutral ($q_X^R = 0$), and we include the renormalizable Yukawa portal $-y_p \bar{\chi}\chi R$. In this realization $U(1)_X$ is unbroken by R acquiring a VEV, so the Z' mass can be generated through a Stückelberg mechanism. The Yukawa interaction $y_p \bar{\chi}\chi R$ controls the coupling of DM to the dark scalar, and since χ is vector-like,

$$m_\chi = m_0 + \frac{y_p v_r}{\sqrt{2}}. \quad (\text{A2})$$

Since R is neutral ($q_X^R = 0$), gauge invariance of the $R \bar{N}^c N$ term implies that the heavy neutrinos N_i are also neutral under $U(1)_X$. Therefore, N_I do not couple to Z' .

The covariant derivative is $D_\mu = \partial_\mu + i q_X g_X Z'_\mu$ (e.g. $q_X \rightarrow q_X^\chi$ on χ). We define $\alpha_X \equiv g_X^2/(4\pi)$. Here $F'_{\mu\nu}$ and g_X denote the field strength and coupling of Z'_μ . The term $-\frac{\epsilon}{2}F'_{\mu\nu}B^{\mu\nu}$ represents kinetic mixing between $U(1)_X$ and hypercharge, controlled by ϵ [38, 39]. SM fermions are neutral under $U(1)_X$, so they couple to Z' only via kinetic mixing at tree level.

2. R – Φ Mixing

The scalar potential is

$$V(\Phi, R) = \mu_H^2 \Phi^\dagger \Phi + \mu_R^2 R^\dagger R + \lambda_H (\Phi^\dagger \Phi)^2 + \lambda_R (R^\dagger R)^2 + \kappa (\Phi^\dagger \Phi)(R^\dagger R). \quad (\text{A3})$$

After EWSB,

$$\Phi = \begin{pmatrix} G^+ \\ \frac{v_h + h + iG^0}{\sqrt{2}} \end{pmatrix}, \quad \tilde{\Phi} = i\sigma_2 \Phi^* = \begin{pmatrix} \frac{v_h + h - iG^0}{\sqrt{2}} \\ -G^- \end{pmatrix}, \quad R = \frac{v_r + \rho}{\sqrt{2}}, \quad (\text{A4})$$

with $v_h \simeq 246$ GeV the SM Higgs vacuum expectation value (VEV) and v_r the singlet VEV; G^+ and G^0 are eaten by W^\pm and Z . Since $U(1)_X$ is unbroken by R , no extra Goldstone appears. In the CP-even basis (h, ρ) ,

$$\mathcal{M}^2 = \begin{pmatrix} 2\lambda_H v_h^2 & \kappa v_h v_r \\ \kappa v_h v_r & 2\lambda_R v_r^2 \end{pmatrix}, \quad \tan 2\alpha = \frac{\kappa v_h v_r}{\lambda_R v_r^2 - \lambda_H v_h^2}, \quad (\text{A5})$$

and the mass eigenstates are

$$\begin{pmatrix} H \\ H_p \end{pmatrix} = \begin{pmatrix} \cos \alpha & \sin \alpha \\ -\sin \alpha & \cos \alpha \end{pmatrix} \begin{pmatrix} h \\ \rho \end{pmatrix}, \quad \Rightarrow \quad h = \cos \alpha H - \sin \alpha H_p, \quad \rho = \sin \alpha H + \cos \alpha H_p, \quad (\text{A6})$$

with masses

$$m_{H, H_p}^2 = \lambda_H v_h^2 + \lambda_R v_r^2 \mp \sqrt{(\lambda_R v_r^2 - \lambda_H v_h^2)^2 + (\kappa v_h v_r)^2}. \quad (\text{A7})$$

3. Interaction Terms in the Mass Basis

We now expand the interaction terms for H, H_p with SM and dark fermions.

a. (i) *SM fermions.* The SM Yukawa Lagrangian $-\mathcal{L} \supset y_f \bar{f}_L \Phi f_R + \text{h.c.}$ with $m_f = y_f v_h / \sqrt{2}$ gives, after EWSB and Eq. (A6),

$$\mathcal{L}_{H, H_p - f\bar{f}} = - \sum_f \frac{m_f}{v_h} (\cos \alpha H - \sin \alpha H_p) \bar{f} f, \quad (\text{A8})$$

so $g_{H_f \bar{f}} = \frac{m_f}{v_h} \cos \alpha$ and $g_{H_p f \bar{f}} = - \frac{m_f}{v_h} \sin \alpha$.

b. (ii) *Dark matter.* From $-\mathcal{L} \supset y_p \bar{\chi} \chi R$,

$$\mathcal{L}_{H, H_p - \chi\bar{\chi}} = - \frac{y_p}{\sqrt{2}} (\sin \alpha H + \cos \alpha H_p) \bar{\chi} \chi, \quad (\text{A9})$$

so $g_{H \chi \bar{\chi}} = \frac{y_p}{\sqrt{2}} \sin \alpha$ and $g_{H_p \chi \bar{\chi}} = \frac{y_p}{\sqrt{2}} \cos \alpha$.

c. (iii) *Heavy (right-handed) neutrinos.* From $-\mathcal{L} \supset \frac{1}{2} Y_N^{ij} R \bar{N}_i^c N_j + \text{h.c.}$ one has $M_N = \frac{v_r}{\sqrt{2}} Y_N$ and

$$\mathcal{L}_{\rho N N} = - \frac{1}{2\sqrt{2}} \rho \bar{N}^c Y_N N + \text{h.c.} \quad (\text{A10})$$

In the heavy-neutrino mass basis, $U_N^T M_N U_N = \widehat{M}_N = \text{diag}(M_1, M_2, M_3)$ and $U_N^T Y_N U_N = \sqrt{2} \widehat{M}_N / v_r$, so

$$\mathcal{L}_{H, H_p - N N} = - \sum_{I=1}^3 \frac{M_I}{2v_r} (\sin \alpha H + \cos \alpha H_p) \bar{N}_I^c N_I + \text{h.c.} \quad (\text{A11})$$

Equivalently, in terms of $y_{N,I}$ with $M_I = y_{N,I} v_r / \sqrt{2}$, $\mathcal{L} \supset - \sum_I \frac{1}{2\sqrt{2}} y_{N,I} (\sin \alpha H + \cos \alpha H_p) \bar{N}_I^c N_I + \text{h.c.}$ Therefore $g_{N_I N_I H_p} = \frac{y_{N,I}}{\sqrt{2}} \cos \alpha$ and $g_{N_I N_I H} = - \frac{m_f}{v_h} \sin \alpha$.

d. (iv) *Light-heavy neutrino Yukawas (Dirac sector).* From $-\mathcal{L} \supset Y_\nu^{\alpha i} \bar{L}_\alpha \tilde{\Phi} N_i + \text{h.c.}$ one obtains $m_D = Y_\nu v_h / \sqrt{2}$ and

$$\mathcal{L}_{H, H_p - \nu N} = - \frac{1}{\sqrt{2}} (\cos \alpha H - \sin \alpha H_p) \bar{\nu}_{L\alpha} Y_\nu^{\alpha i} N_i + \text{h.c.}, \quad (\text{A12})$$

which directly gives the H, H_p couplings to light-heavy pairs in the mass basis (see also Sec. B 4 for the aligned limit). The light-heavy neutrino couplings are encoded in Y_ν as they appear in Eq. (A12); they are generally non-diagonal and become diagonal only in the aligned limit (Sec. B 4).

e. (v) *Scalar potential (for reference).* From $V(\Phi, R) = \mu_H^2 \Phi^\dagger \Phi + \mu_R^2 R^\dagger R + \lambda_H (\Phi^\dagger \Phi)^2 + \lambda_R (R^\dagger R)^2 + \kappa (\Phi^\dagger \Phi)(R^\dagger R)$, the cubic interactions in the gauge basis are

$$V_{\text{cubic}} \supset \lambda_H v_h h^3 + \lambda_R v_r \rho^3 + \frac{\kappa}{2} v_h h \rho^2 + \frac{\kappa}{2} v_r h^2 \rho. \quad (\text{A13})$$

Using Eq. (A6) one can obtain all H, H_p trilinears (e.g. HHH , HHH_p , $HH_p H_p$, $H_p H_p H_p$). These are relevant for scalar cascades and self-scattering but not needed for the fermionic interactions above.

4. Useful Decay Rates and Annihilation Cross Sections

a. Decay rate of H_p

The couplings in Sec. A 3 fix the tree-level partial widths of H_p into fermion pairs. For a Dirac fermion f with $\mathcal{L} \supset -g_{H_p f \bar{f}} H_p \bar{f} f$,

$$\Gamma(H_p \rightarrow f \bar{f}) = N_c^f \frac{g_{H_p f \bar{f}}^2}{8\pi} m_{H_p} \left(1 - \frac{4m_f^2}{m_{H_p}^2} \right)^{3/2}, \quad (\text{A14})$$

where N_c^f is the color factor. Using $g_{H_p f \bar{f}} = -(m_f/v_h) \sin \alpha$,

$$\Gamma_{\text{ferm}}(H_p) = \sum_f \frac{N_c^f m_{H_p}}{8\pi} \frac{m_f^2}{v_h^2} \sin^2 \alpha \left(1 - \frac{4m_f^2}{m_{H_p}^2}\right)^{3/2}, \quad (\text{A15})$$

summing over all kinematically allowed f with $m_{H_p} > 2m_f$.

For the DM channel, $g_{H_p \chi \bar{\chi}} = \frac{y_p}{\sqrt{2}} \cos \alpha$ gives (for $m_{H_p} > 2m_\chi$)

$$\Gamma(H_p \rightarrow \chi \bar{\chi}) = \frac{y_p^2 \cos^2 \alpha}{16\pi} m_{H_p} \left(1 - \frac{4m_\chi^2}{m_{H_p}^2}\right)^{3/2}. \quad (\text{A16})$$

If open, heavy-neutrino final states $H_p \rightarrow N_I N_I$ contribute with $g_{H_p N_I N_I} = \frac{y_{N,I}}{\sqrt{2}} \cos \alpha$ (Majorana prefactor understood). In the parameter region of interest, the branching ratios are controlled by the competition between the mixing-suppressed SM channels $\propto \sin^2 \alpha$ and the direct dark-portal channel $\propto y_p^2 \cos^2 \alpha$. For small α and $m_{H_p} > 2m_\chi$, one typically has $\text{BR}(H_p \rightarrow \chi \bar{\chi}) \simeq 1$, unless sizable $H_p \rightarrow N_I N_I$ is kinematically allowed.

b. Tree-level $\chi \bar{\chi} \rightarrow H_p H_p$ and the p -wave coefficient

We take a Dirac fermion χ of mass m_χ coupled to a real scalar H_p of mass m_{H_p} via

$$\mathcal{L} \supset y_p \bar{\chi} \chi H_p. \quad (\text{A17})$$

The thermal average cross section comes from the t/u diagrams, it is p -wave and given by the following expression

$$\sigma v_{\text{rel}}(\chi \bar{\chi} \rightarrow H_p H_p) = \frac{y_p^4}{64\pi m_\chi^2} \frac{\sqrt{1-r}}{\left(1 - \frac{r}{2}\right)^4} \left(1 - r + \frac{r^2}{8}\right) v_{\text{rel}}^2 + \mathcal{O}(v_{\text{rel}}^4), \quad (\text{A18})$$

where $r = m_{H_p}^2/m_\chi^2$.

Appendix B: Light and heavy neutrino masses, interactions, and the seesaw mechanism

In this appendix we explain the setup for the light and heavy neutrino Yukawa couplings, masses, and the type-I seesaw mechanism. In Sec. B 1 we discuss the Yukawa interactions of light and heavy neutrinos with the scalars; in Sec. B 2 we report the main steps of the type-I seesaw mechanism; and in Sec. B 3 we list the couplings in the mass eigenstate basis. The details of the neutrino Yukawa interactions and the seesaw mechanism are inspired by Refs. [40, 50–53].

1. Light and heavy neutrino Yukawa interactions

The interactions between light and heavy neutrinos and the scalars Φ and R are given in Eq. (A1):

$$\mathcal{L}_Y \supset -Y_\nu^{\alpha i} \overline{L_\alpha} \tilde{\Phi} N_i - \frac{1}{2} Y_N^{ij} R \overline{N_i^c} N_j + \text{h.c.}, \quad (\text{B1})$$

where L_α are the left-handed lepton doublets (with $\alpha = e, \mu, \tau$ labelling lepton flavours), $i, j = 1, 2, 3$ label right-handed singlet neutrinos, Y_ν is a generic complex 3×3 matrix, and $Y_N = Y_N^T$ is complex symmetric.

Dirac term. After EWSB the first term in Eq. (B1) can be written as

$$-Y_\nu^{\alpha i} \overline{L_\alpha} \tilde{\Phi} N_i = -Y_\nu^{\alpha i} \left[\overline{\nu_{\alpha L}} \frac{v_h + h - iG^0}{\sqrt{2}} - \overline{\ell_{\alpha L}} G^- \right] N_i. \quad (\text{B2})$$

Focusing on the neutral part and switching to matrix notation,

$$-\overline{\nu_L} \frac{v_h + h - iG^0}{\sqrt{2}} Y_\nu N + \text{h.c.} = -\overline{\nu_L} \underbrace{\left(\frac{v_h}{\sqrt{2}} Y_\nu \right)}_{m_D} N - \frac{1}{\sqrt{2}} \overline{\nu_L} h Y_\nu N + \frac{i}{\sqrt{2}} \overline{\nu_L} G^0 Y_\nu N + \text{h.c.} \quad (\text{B3})$$

We identify in the Dirac mass term $-\overline{\nu_L} m_D N$ the 3×3 Dirac mass matrix $m_D \equiv v_h Y_\nu / \sqrt{2}$. The remaining terms in Eq. (B3) describe the couplings of ν_L to the physical Higgs field h and to the neutral Goldstone G^0 .

Majorana term. For the singlet sector, one has

$$-\frac{1}{2} Y_N^{ij} R \overline{N_i^c} N_j = -\frac{1}{2} \frac{v_r + \rho}{\sqrt{2}} Y_N^{ij} \overline{N_i^c} N_j = -\frac{1}{2} \overline{N^c} \left(\underbrace{\frac{v_r}{\sqrt{2}} Y_N}_{M_N} \right) N - \frac{1}{2\sqrt{2}} \overline{N^c} \rho Y_N N. \quad (\text{B4})$$

Thus from the Majorana mass term $-\frac{1}{2} \overline{N^c} M_N N$, we identify the heavy-neutrino Majorana mass matrix $M_N \equiv v_r Y_N / \sqrt{2}$, which is complex symmetric, and the coupling of ρ to $N_i N_j$ is proportional to Y_N .

2. Type-I seesaw mechanism

Collecting the VEV-induced pieces, the neutral-fermion mass Lagrangian is

$$\mathcal{L}_{\text{mass}} \supset -\overline{\nu_L} m_D N - \frac{1}{2} \overline{N^c} M_N N + \text{h.c.} \quad (\text{B5})$$

It is convenient to write this in a symmetric 6×6 form. Define

$$n_L \equiv \begin{pmatrix} \nu_L \\ N^c \end{pmatrix}, \quad n_L^c = \begin{pmatrix} \nu_L^c \\ N \end{pmatrix}. \quad (\text{B6})$$

Using $\overline{\nu_L} m_D N = \frac{1}{2} (\overline{\nu_L} m_D N + \overline{N^c} m_D^T \nu_L^c)$ and similarly for the Majorana term, we obtain

$$\mathcal{L}_{\text{mass}} \supset -\frac{1}{2} \overline{n_L^c} \mathcal{M} n_L + \text{h.c.}, \quad \mathcal{M} = \begin{pmatrix} 0 & m_D \\ m_D^T & M_N \end{pmatrix}, \quad (\text{B7})$$

where \mathcal{M} is complex symmetric, as appropriate for Majorana masses.

Type-I seesaw: matrix diagonalization. In the seesaw regime $\|m_D M_N^{-1}\| \ll 1$, we define

$$\Theta \equiv m_D M_N^{-1}, \quad (\text{B8})$$

and the block-antihermitian generator

$$\Omega = \begin{pmatrix} 0 & \Theta \\ -\Theta^\dagger & 0 \end{pmatrix}, \quad (\text{B9})$$

which can be used to approximately block-diagonalize \mathcal{M} via an (approximately) unitary transformation $U_I \simeq \exp(-\Omega)$. To second order in Θ one finds

$$U_I^T \mathcal{M} U_I = \begin{pmatrix} M_\nu & 0 \\ 0 & M_{\text{heavy}} \end{pmatrix} + \mathcal{O}(\Theta^3), \quad (\text{B10})$$

with

$$M_\nu = -m_D M_N^{-1} m_D^T = -\Theta M_N \Theta^T + \mathcal{O}(\Theta^4 M_N), \quad (\text{B11})$$

$$M_{\text{heavy}} = M_N + \frac{1}{2} (\Theta^\dagger m_D + m_D^T \Theta) + \mathcal{O}(\Theta^4 M_N). \quad (\text{B12})$$

Thus $M_{\text{heavy}} \simeq M_N$ up to relative $\mathcal{O}(\Theta^2)$ corrections.

In the one-generation case with real parameters m_D and M_N , the eigenvalues are

$$m_{\text{light}} \simeq -\frac{m_D^2}{M_N}, \quad m_{\text{heavy}} \simeq M_N \left(1 + \frac{m_D^2}{M_N^2} \right). \quad (\text{B13})$$

In terms of the Yukawa couplings, using $m_D = y_\nu v_h / \sqrt{2}$ and $M_N = y_N v_r / \sqrt{2}$, the seesaw relation for one generation can be written as

$$m_\nu \simeq -\frac{m_D^2}{M_N} = -\frac{y_\nu^2 v_h^2}{\sqrt{2} y_N v_r}, \quad M_{\text{heavy}} \simeq M_N = \frac{y_N v_r}{\sqrt{2}}. \quad (\text{B14})$$

3. Light and heavy neutrino mass eigenstates and Yukawa interactions in this basis

Heavy (RH) neutrino mass eigenstates. Since M_N is complex symmetric, it admits a Takagi factorization: there exists a unitary matrix U_N such that

$$U_N^T M_N U_N = \widehat{M}_N \equiv \text{diag}(M_1, M_2, M_3), \quad M_I > 0. \quad (\text{B15})$$

We define the heavy-neutrino mass eigenstates N_I via

$$N_i = (U_N)_{iI} N_I, \quad (\text{B16})$$

so that the mass term becomes

$$\mathcal{L}_M \supset -\frac{1}{2} \overline{N^c} M_N N = -\frac{1}{2} \overline{N^c}_I (U_N^T M_N U_N)_{IJ} N_J = -\frac{1}{2} \sum_I M_I \overline{N^c}_I N_I. \quad (\text{B17})$$

Equivalently, in terms of the diagonal Yukawas,

$$\widehat{Y}_N \equiv U_N^T Y_N U_N = \text{diag}(y_{1,N}, y_{2,N}, y_{3,N}), \quad M_I = \frac{v_r}{\sqrt{2}} y_{I,N}. \quad (\text{B18})$$

In this basis (\widehat{M}_N diagonal), the Dirac mass matrix becomes

$$m_D \rightarrow m'_D = m_D U_N = \frac{v_h}{\sqrt{2}} Y'_\nu, \quad Y'_\nu \equiv Y_\nu U_N, \quad (\text{B19})$$

which is generically non-diagonal.

Light neutrinos and type-I seesaw. In the basis with diagonal \widehat{M}_N , the seesaw formula (B11) reads

$$M_\nu \simeq -m_D M_N^{-1} m_D^T = -m'_D \widehat{M}_N^{-1} m_D^T = -\frac{v_h^2}{2} Y'_\nu \widehat{M}_N^{-1} Y'^T_\nu. \quad (\text{B20})$$

The light-neutrino mass matrix M_ν is complex symmetric and is diagonalized by a unitary matrix U_ν :

$$U_\nu^T M_\nu U_\nu = \widehat{m}_\nu \equiv \text{diag}(m_1, m_2, m_3), \quad m_i \geq 0. \quad (\text{B21})$$

The light-neutrino mass eigenstates ν_i are defined by

$$\nu_{L\alpha} = (U_\nu)_{\alpha i} \nu_{iL}, \quad (\text{B22})$$

up to rephasings; U_ν can be identified with the PMNS matrix in the usual way.

Yukawa interactions in the mass basis. From Eq. (B3) and the (h, ρ) – (H, H_p) mixing in Eq. (A6), the couplings of the CP-even scalars to ν and N in the flavour basis are

$$\mathcal{L}_{H, H_p - \nu N} = -\frac{1}{\sqrt{2}} (\cos \alpha H - \sin \alpha H_p) \overline{\nu_{L\alpha}} Y_\nu^{\alpha i} N_i + \text{h.c.} \quad (\text{B23})$$

We now rotate to the light and heavy mass bases using Eqs. (B16) and (B22), obtaining

$$\mathcal{L}_{H, H_p - \nu N} = -\frac{1}{\sqrt{2}} (\cos \alpha H - \sin \alpha H_p) \overline{\nu_{iL}} (Y_\nu^{\text{mass}})_{iI} N_I + \text{h.c.}, \quad (\text{B24})$$

where

$$Y_\nu^{\text{mass}} \equiv U_\nu^\dagger Y_\nu U_N. \quad (\text{B25})$$

In general, Y_ν^{mass} is *not* diagonal. The couplings

$$g_H \nu_i N_I = -\frac{\cos \alpha}{\sqrt{2}} (Y_\nu^{\text{mass}})_{iI}, \quad g_{H_p} \nu_i N_I = +\frac{\sin \alpha}{\sqrt{2}} (Y_\nu^{\text{mass}})_{iI}, \quad (\text{B26})$$

show that each heavy neutrino N_I couples to all light eigenstates ν_i .

4. Casas–Ibarra parametrization and aligned limit

Given the low-energy neutrino data (i.e. the light eigenvalues m_i and the PMNS matrix U_ν , including CP phases) and a choice of heavy-neutrino masses M_I (the eigenvalues of M_N), the most general Dirac mass matrix m_D reproducing the type-I seesaw relation

$$M_\nu = -m_D M_N^{-1} m_D^T \quad (\text{B27})$$

can be written in the Casas–Ibarra form

$$m_D = i U_\nu \sqrt{\hat{m}_\nu} O \sqrt{\hat{M}_N}, \quad O^T O = \mathbb{1}, \quad (\text{B28})$$

where

$$\hat{m}_\nu = \text{diag}(m_1, m_2, m_3), \quad \hat{M}_N = \text{diag}(M_1, M_2, M_3), \quad (\text{B29})$$

and O is a complex orthogonal matrix encoding the residual high-energy freedom not fixed by low-energy observables.

In general O is not diagonal, so Eq. (B25) shows that Y_ν^{mass} has off-diagonal entries: each heavy state N_I couples to *all* light mass eigenstates ν_i . Consequently, the seesaw relation $M_\nu = -m_D M_N^{-1} m_D^T$ involves coherent sums over I , and one cannot identify a light mass m_i with a single Yukawa coupling via a simple $m_i = y_{i,\nu} v_h / \sqrt{2}$.

A special simplification occurs only in an *aligned limit*. Work in the basis where the heavy-neutrino mass matrix is diagonal, $M_N = \hat{M}_N = \text{diag}(M_1, M_2, M_3)$, and write the Dirac Yukawas in the light- and heavy-mass bases as

$$Y_\nu^{\text{mass}} = i \frac{\sqrt{2}}{v_h} \sqrt{\hat{m}_\nu} O \sqrt{\hat{M}_N}, \quad (\text{B30})$$

with $\hat{m}_\nu = \text{diag}(m_1, m_2, m_3)$ and O a complex orthogonal matrix. For generic O the matrix Y_ν^{mass} is not diagonal, so each light eigenstate ν_i couples to several heavy states N_I and its mass m_i arises from a coherent combination of $(Y_\nu^{\text{mass}})_{iI}$ entries. In this generic situation it is *not* correct to write $m_i = y_{i,\nu} v_h / \sqrt{2}$ with a single Yukawa $y_{i,\nu}$.

In contrast, in the aligned limit we choose

$$O = \mathbb{1}, \quad (\text{B31})$$

and use the freedom to relabel the heavy mass eigenstates so that the indices of \hat{m}_ν and \hat{M}_N are paired consistently. Then Eq. (B30) reduces to

$$Y_\nu^{\text{mass}} = i \frac{\sqrt{2}}{v_h} \sqrt{\hat{m}_\nu} \sqrt{\hat{M}_N} = i \text{diag}\left(\frac{\sqrt{2m_1 M_1}}{v_h}, \frac{\sqrt{2m_2 M_2}}{v_h}, \frac{\sqrt{2m_3 M_3}}{v_h}\right). \quad (\text{B32})$$

Therefore, in the aligned limit ($O = \mathbb{1}$ with a consistent pairing of $m_{\nu,I}$ and M_I), the Yukawa matrix in the mass basis is diagonal and one finds

$$y_{I,\nu} \equiv (Y_\nu^{\text{mass}})_{II} = \frac{\sqrt{2m_{\nu,I} M_I}}{v_h}. \quad (\text{B33})$$

In this case the type-I seesaw relation holds pairwise,

$$m_{\nu,I} = \frac{v_h^2}{2} \frac{|y_{I,\nu}|^2}{M_I}. \quad (\text{B34})$$

Outside this special aligned limit ($O \neq \mathbb{1}$ and/or a different labelling of the heavy eigenstates), Y_ν^{mass} is non-diagonal and each m_i is generated by several entries $(Y_\nu^{\text{mass}})_{iI}$. One must then retain the full matrix structure of Y_ν^{mass} (equivalently, m_D) in the seesaw relation, and the naive identification $m_i = y_{i,\nu} v_h / \sqrt{2}$ for the light states is not valid.

Appendix C: Thermal averaging and effective rates

In a radiation-dominated expanding Universe, departures of the number density of a species X from equilibrium relax back with an *effective* rate that sums all number-changing channels that create or destroy X , normalized to the equilibrium abundance. Linearizing the Boltzmann equation around n_X^{eq} ,

$$\dot{n}_X + 3Hn_X = -(n_X - n_X^{\text{eq}}) \Gamma_X^{\text{eff}}(T), \quad \Gamma_X^{\text{eff}}(T) = \frac{\sum_i \gamma_i(T)}{n_X^{\text{eq}}(T)}, \quad (\text{C1})$$

where the sum runs over all relevant processes i and γ_i are the corresponding reaction densities (rates per unit volume). Chemical equilibrium is maintained when $\Gamma_X^{\text{eff}} \gg H$. A practical tracking criterion that accounts for the explicit temperature dependence of n_X^{eq} is

$$\frac{\Gamma_X^{\text{eff}}(T)}{H(T)} \gg \frac{3}{2} + \xi_X, \quad \xi_X \equiv \frac{m_X}{T}. \quad (\text{C2})$$

This follows from linearizing the Boltzmann equation and demanding that the relaxation time is much shorter than the Hubble time, including the dilution term. However, in the paper we have just used the simplified condition $\frac{\Gamma_X^{\text{eff}}(T)}{H(T)} \gg 1$.

a. *Reaction densities and reduced cross sections.* For a generic $2 \rightarrow 2$ process $ab \rightarrow cd$, the reaction density is

$$\gamma_{ab \rightarrow cd}(T) = \int d\Pi_a d\Pi_b d\Pi_c d\Pi_d (2\pi)^4 \delta^{(4)}(p_a + p_b - p_c - p_d) f_a^{\text{eq}} f_b^{\text{eq}} (1 \pm f_c^{\text{eq}}) (1 \pm f_d^{\text{eq}}) |\mathcal{M}_{ab \rightarrow cd}|^2, \quad (\text{C3})$$

with $d\Pi_i \equiv d^3 p_i / [(2\pi)^3 2E_i]$ and $f_{F,B}^{\text{eq}}(E) = 1/(e^{E/T} \pm 1)$ for fermions/bosons. Using standard manipulations and introducing the reduced cross section $\hat{\sigma} \equiv 2s\sigma$ (see, e.g., [50, 54–56]), this can be written for (effectively) massless initial states as

$$\gamma_{ab \rightarrow cd}(T) = \frac{T}{64\pi^4} \int_{s_{\min}}^{\infty} ds \hat{\sigma}_{ab \rightarrow cd}(s) \sqrt{s} K_1\left(\frac{\sqrt{s}}{T}\right), \quad (\text{C4})$$

where K_1 is a modified Bessel function and s_{\min} includes thermal masses when relevant. Quantum–statistical factors and thermal corrections are encoded in $\hat{\sigma}$ and in the effective threshold s_{\min} .

When Maxwell–Boltzmann factorization holds one may also estimate $\gamma_{ab \rightarrow cd} \simeq n_a^{\text{eq}} n_b^{\text{eq}} \langle \sigma v \rangle$; Eqs. (C3)–(C4) provide the exact thermal result used in our calculations.

Useful templates

b. (i) *Pair annihilation $XX \leftrightarrow \text{SM}$.* Near equilibrium,

$$\dot{n}_X + 3Hn_X = -\langle \sigma v \rangle (n_X^2 - n_X^{\text{eq}})^2 \Rightarrow \Gamma_X^{\text{eff}} = 2 \langle \sigma v \rangle n_X^{\text{eq}}. \quad (\text{C5})$$

(The factor 2 counts the two X destroyed per reaction.)

c. (ii) *Semi-annihilation $XX \leftrightarrow XY$.*

$$\Gamma_X^{\text{eff}} = \langle \sigma v \rangle n_X^{\text{eq}}. \quad (\text{C6})$$

d. (iii) *Coannihilation $Xa \leftrightarrow \text{SM}$ (partner a thermal).*

$$\Gamma_X^{\text{eff}} \simeq \langle \sigma v \rangle_{Xa} n_a^{\text{eq}}. \quad (\text{C7})$$

e. (iv) *Decay / inverse decay $X \leftrightarrow \text{SM}$.*

$$\Gamma_X^{\text{eff}} = \Gamma_D \frac{K_1(\xi_X)}{K_2(\xi_X)}, \quad \xi_X \equiv \frac{m_X}{T}, \quad (\text{C8})$$

with $K_1/K_2 \simeq \xi_X/2$ for $\xi_X \ll 1$ and $K_1/K_2 \rightarrow 1$ for $\xi_X \gg 1$.

f. (v) *$2 \rightarrow 2$ production of a single X : $ab \rightarrow X \dots$*

$$\Gamma_X^{\text{eff}} = \frac{\gamma_{ab \rightarrow X \dots}(T)}{n_X^{\text{eq}}(T)}, \quad (\text{C9})$$

with γ from Eq. (C4). This is the precise counterpart of the heuristic $\Gamma \sim \sum n^{\text{eq}} \langle \sigma v \rangle$.

g. (vi) *Number-changing $3 \rightarrow 2$.*

$$\dot{n}_X + 3Hn_X = -\langle \sigma v^2 \rangle (n_X^3 - n_X^{\text{eq}})^3 \Rightarrow \Gamma_X^{\text{eff}} = 3 \langle \sigma v^2 \rangle (n_X^{\text{eq}})^2. \quad (\text{C10})$$

h. (vii) *Elastic (kinetic) scattering with bath species b .*

$$\Gamma_{\text{kin}} \simeq n_b^{\text{eq}} \langle \sigma_T v \rangle, \quad (\text{C11})$$

relevant for temperature (rather than number) equilibration.

In natural units, $n^{\text{eq}} \sim \text{GeV}^3$ and $\gamma \sim \text{GeV}^4$, hence $\Gamma^{\text{eff}} = \gamma/n^{\text{eq}} \sim \text{GeV}$. Boltzmann and threshold effects are automatically encoded in Eqs. (C3)–(C4) and in $K_1(\xi_X)/K_2(\xi_X)$; as a result, Γ^{eff}/H drops rapidly once $\xi_X \gtrsim \mathcal{O}(1\text{--}3)$.

Appendix D: Details of $\Delta L = 1$ Scatterings at High Temperature

As discussed in the main text, for temperatures larger than the lightest heavy-neutrino mass, $T \gtrsim M_N$, the SM bath is in thermal contact with the hidden sector through the neutrino portal. In this section, H denotes the SM Higgs doublet in the unbroken phase, not the CP-even mass eigenstate H of App. A.

The relevant interaction terms are

$$-\mathcal{L}_Y \supset Y_\nu^{\alpha I} \overline{L_\alpha} \tilde{H} N_I + \frac{1}{2} Y_N^{IJ} R \overline{N_I^c} N_J + y_p \bar{\chi} \chi R + y_t \overline{Q_3} \tilde{H} t_R + \text{h.c.}, \quad (\text{D1})$$

$$\mathcal{L}_{\text{gauge}} \supset \sum_f \bar{f} \gamma^\mu (g_2 T^a W_\mu^a + g_Y Y B_\mu) f + (D_\mu H)^\dagger (D^\mu H) + \bar{\chi} i \gamma^\mu (\partial_\mu + i g_X q_\chi Z_\mu') \chi, \quad (\text{D2})$$

with $\tilde{H} = i \sigma_2 H^*$, f running over SM fermions, T^a the $SU(2)_L$ generators, Y hypercharge, and D_μ the SM covariant derivative acting on H . The process Feynman diagrams are reported in Fig. 4. We list below the main processes keeping the hidden sector in thermal contact with the SM:

(i) *Decays and inverse decays* (with violation of lepton number $\Delta L = 1$):

$$N_I \leftrightarrow L_\alpha H, \quad N_I \leftrightarrow \bar{L}_\alpha H^\dagger. \quad (\text{D3})$$

These control the production and destruction of heavy neutrinos N_I and are the leading neutrino–portal processes in the relativistic and mildly non–relativistic regimes.

(ii) $\Delta L = 1$ *Yukawa–mediated scatterings* with one Y_ν and one SM coupling, e.g.

$$N_I L_\alpha \leftrightarrow Q_3 t, \quad L_\alpha A \leftrightarrow N_I H, \quad (\text{D4})$$

and their crossed channels, mediated by Higgs or lepton exchange, where A is a SM electroweak gauge boson. These are $\mathcal{O}(Y_\nu^2 y_t^2)$ and $\mathcal{O}(Y_\nu^2 g^2)$ processes and efficiently contribute to keeping N_I in kinetic and chemical contact with the SM plasma for $T \gtrsim M_I$.

(iii) $\Delta L = 2$ *scatterings* induced by virtual N_I , such as

$$L_\alpha H \leftrightarrow \bar{L}_\beta H^\dagger, \quad L_\alpha L_\beta \leftrightarrow H H, \quad (\text{D5})$$

which encode lepton–number violation and are relevant for washout and for the low-energy Weinberg operator once N_I are integrated out. These processes are relevant only at very high temperatures ($T \gtrsim 10^{12}$ GeV) and are negligible near (and below) $T \sim M_I$. We will not consider them further.

(iv) *Portal processes involving the dark scalar and DM*, mediated by N_I and R , e.g.

$$N_I N_J \leftrightarrow R, \quad N_I R \leftrightarrow L_\alpha H, \quad R R \leftrightarrow H H, \quad (\text{D6})$$

and, via the R – χ coupling, reactions that transfer energy and number between χ and the SM through the N_I – R chain. Once N_I are in equilibrium with the SM, these interactions help ensure that the dark sector is also thermally linked.

In the following we quantify the rates of decays/inverse decays, the leading $\Delta L = 1$ scatterings, and the portal processes involving the dark scalar and DM. We work in the unbroken phase and for $T \gg m_{\text{EW}}$, taking all external masses (except $M_{N,I}$) negligible. When several heavy Majorana eigenstates N_I are present, the slowest (last) to lose equilibrium is the *lightest* one. It is therefore sufficient (and conservative) to track a single state N with mass $M_N \equiv \min_I(M_{N,I})$. In the aligned limit, we denote by m_ν the light eigenvalue paired with this lightest N .

1. Tree-level width $N_I \rightarrow L_\alpha H$

We start from the neutrino Yukawa interaction for a given mass eigenstate N_I ,

$$\mathcal{L}_{\text{int}} \supset -y_{\alpha I} \overline{L_\alpha} \tilde{H} N_I + \text{h.c.}$$

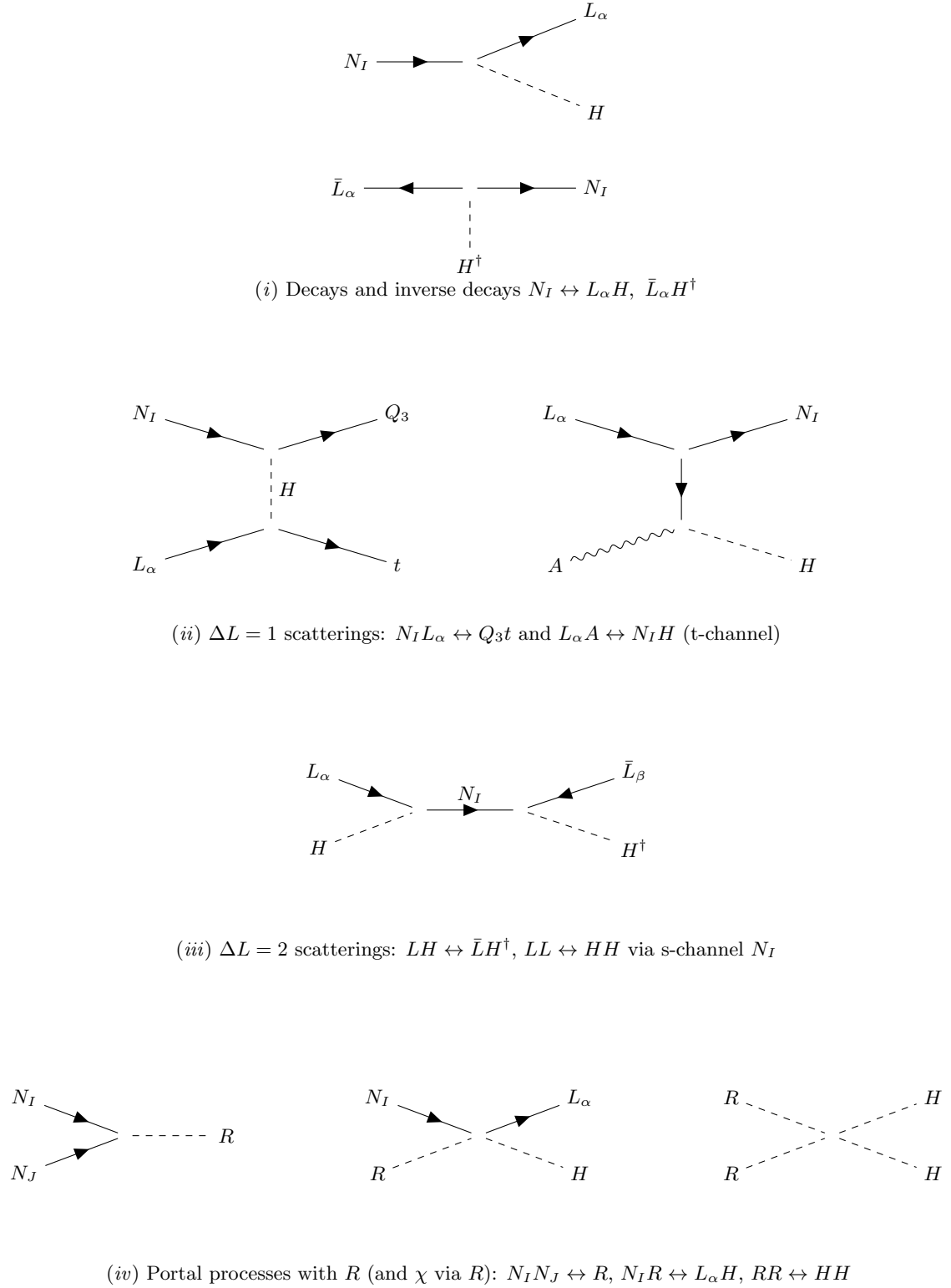


FIG. 4. Representative neutrino-portal processes maintaining thermal contact between the SM, the heavy neutrinos N_I , and the dark sector at $T \gg M_I$.

Expanding in components, this contains decays of the form $N_I \rightarrow \ell_\alpha H$. Summing over lepton flavours yields the total width for decays and inverse decays

$$\Gamma_{D,I} \equiv \Gamma(N_I \rightarrow LH) + \Gamma(N_I \rightarrow \bar{L}H^\dagger) = \frac{M_{N,I}}{8\pi} \sum_\alpha |y_{\alpha I}|^2 \mathcal{F}(r_H, r_{\ell_\alpha}), \quad (\text{D7})$$

with

$$\mathcal{F}(r_H, r_{\ell_\alpha}) = \sqrt{(1 - r_H - r_{\ell_\alpha})^2 - 4r_H r_{\ell_\alpha}} (1 + r_{\ell_\alpha} - r_H), \quad r_H \equiv \frac{m_H^2}{M_{N,I}^2}, \quad r_{\ell_\alpha} \equiv \frac{m_{\ell_\alpha}^2}{M_{N,I}^2}. \quad (\text{D8})$$

In the unbroken phase, or whenever $M_{N,I} \gg m_H, m_{\ell_\alpha}$, $\mathcal{F}(r_H, r_{\ell_\alpha}) \rightarrow 1$, so that

$$\Gamma_{D,I} = \frac{M_{N,I}}{8\pi} (y^\dagger y)_{II}. \quad (\text{D9})$$

This is the standard expression used in leptogenesis analyses [48–50].

In the early Universe the heavy neutrinos N_I are immersed in a thermal bath and are produced with a momentum distribution rather than at rest. The relevant quantity for equilibration is the *time-dilated*, thermally averaged decay rate per particle (see App. C) for the lightest of the heavy neutrinos N ,

$$\langle \Gamma_D \rangle_T = \Gamma_D \frac{K_1(\xi)}{K_2(\xi)}, \quad \xi \equiv \frac{M_N}{T}, \quad (\text{D10})$$

where $K_{1,2}$ are modified Bessel functions of the second kind and we assume Maxwell–Boltzmann statistics for N_I . To assess thermal contact we compare $\langle \Gamma_D \rangle_T$ with the Hubble rate during radiation domination,

$$H(T) = 1.66 \sqrt{g_*(T)} \frac{T^2}{M_{\text{Pl}}} = 1.66 \sqrt{g_*} \frac{M_N^2}{M_{\text{Pl}}} \frac{1}{\xi^2}, \quad (\text{D11})$$

where g_* is the effective number of relativistic degrees of freedom. Using Eqs. (D10) and (D9) and in the aligned Casas–Ibarra limit ($(y^\dagger y)_{II} = 2m_{\nu,I}M_I/v_h^2$) the ratio $\langle \Gamma_{D,I} \rangle_T / H(T)$ simplifies to

$$\frac{\langle \Gamma_D \rangle_T}{H(T)} = \frac{m_\nu M_{\text{Pl}}}{4\pi 1.66 \sqrt{g_*} v_h^2} \xi^2 \frac{K_1(\xi)}{K_2(\xi)}. \quad (\text{D12})$$

We define the equilibration (or decoupling) temperature T_* by

$$\left. \frac{\langle \Gamma_D \rangle_T}{H(T)} \right|_{T=T_*} = 1. \quad (\text{D13})$$

For $T_* \gg M_N$ (i.e. $\xi_* \ll 1$), we can use $K_1(\xi)/K_2(\xi) \simeq \xi/2$, so Eq. (D12) yields

$$\frac{T_*}{M_N} \simeq 2.8 \left(\frac{m_\nu}{0.05 \text{ eV}} \right)^{1/3} \left(\frac{106.75}{g_*} \right)^{1/6}, \quad (\text{D14})$$

so that N enter equilibrium as the Universe cools to $T \sim \text{few} \times M_N$, and are well in equilibrium for $T \lesssim \text{few} \times M_N$. Evaluating Eq. (D12) at $T = M_N$ ($\xi = 1$) gives

$$\left. \frac{\langle \Gamma_D \rangle_T}{H(T)} \right|_{T=M_N} = \frac{m_\nu M_{\text{Pl}}}{4\pi 1.66 \sqrt{g_*} v_h^2} \frac{K_1(1)}{K_2(1)} \sim \mathcal{O}(20\text{--}30) \quad \text{for } m_\nu \sim 0.05 \text{ eV}, \quad (\text{D15})$$

confirming that decays and inverse decays alone are fast enough to maintain thermal contact around and below $T \sim \text{few} \times M_N$ for seesaw–motivated parameters.

Top-assisted scattering $N_I L_\alpha \rightarrow Q_3 t$

We now consider the process $N_I(p_1) + L_\alpha(p_2) \rightarrow Q_3(p_3) + t(p_4)$ mediated by t -channel Higgs exchange of the interaction term $-\mathcal{L} \supset y_{\alpha I} \overline{L_\alpha} \tilde{H} N_I + y_t \overline{Q_3} H t_R + \text{h.c.}$. In the relativistic regime $s \gg M_I^2, m_H^2(T)$, after spin/color sums and angular integration one finds a reduced cross section of the form

$$\hat{\sigma}_{N_I L \rightarrow Q_3 t}(s) \equiv 2s \sigma_{N_I L \rightarrow Q_3 t}(s) = \frac{3}{8\pi} (Y_\nu^\dagger Y_\nu)_{II} |y_t|^2 \mathcal{F}_t \left(\frac{s}{m_H^2(T)} \right), \quad (\text{D16})$$

with

$$\mathcal{F}_t(x) \equiv \left(1 + \frac{2}{x} \right) \ln(1+x) - 2, \quad x \equiv \frac{s}{m_H^2(T)}. \quad (\text{D17})$$

With Hard Thermal Loop (HTL) thermal masses³ $m_H^2(T) \sim c_H g^2 T^2$ and typical $s \sim (2T)^2$ one has $x = \mathcal{O}(5-20)$, so numerically $\mathcal{F}_t(x) \sim 0.3-1.0$. A fully resummed derivation (including HTL propagators and exact \mathcal{F}_t) can be found in [54–56].

Gauge-assisted scattering $L_\alpha A \rightarrow N_I H$

Now we focus on the process $L_\alpha(p_1) + A(p_2) \rightarrow N_I(p_3) + H(p_4)$ where A is an electroweak gauge boson (W_a or B). These channels involve one neutrino Yukawa and one gauge vertex and are representative of $\mathcal{O}(Y_\nu^2 g^2)$ scatterings. In the unbroken phase the relevant interactions are

$$-\mathcal{L}_Y \supset Y_\nu^{\alpha I} \overline{L_\alpha} \tilde{H} N_I + \text{h.c.}, \quad (\text{D18})$$

$$\mathcal{L}_{\text{gauge}} \supset g \bar{L}_\alpha \gamma^\mu T^a L_\alpha A_\mu^a + (D_\mu H)^\dagger (D^\mu H), \quad (\text{D19})$$

with analogous hypercharge couplings. A representative contribution is the t -channel lepton exchange; s - and u -channel diagrams complete the gauge-invariant set and yield the same parametric dependence once summed.

Summing over spins, polarizations and gauge indices, and working in the relativistic regime $s \gg M_I^2, m_{L,H,A}^2(T)$, one obtains the reduced cross section

$$\hat{\sigma}_{LA \rightarrow N_I H}(s) \equiv 2s \sigma_{LA \rightarrow N_I H}(s) = \frac{C_A}{8\pi} |Y_\nu^{\alpha I}|^2 g^2 \mathcal{F}_g \left(\frac{s}{m_{\text{th}}^2(T)} \right), \quad (\text{D20})$$

where: $C_A = \mathcal{O}(1)$ is a group-theory factor, $m_{\text{th}}^2(T)$ is a representative thermal scale built from $m_L^2(T), m_H^2(T), m_A^2(T)$, and \mathcal{F}_g is a dimensionless function encoding angular structure and IR regularization. A convenient parametrization with the correct limits is

$$\mathcal{F}_g(x) \equiv \left(1 + \frac{1}{x} \right) \ln(1+x) - 1, \quad x \equiv \frac{s}{m_{\text{th}}^2(T)}, \quad (\text{D21})$$

For $m_{\text{th}}^2(T) \sim c g^2 T^2$ and $s \sim (2T)^2$ one typically has $x = \mathcal{O}(5-30)$ and hence $\mathcal{F}_g(x) \sim 0.5-2$. Summing over flavours,

$$\hat{\sigma}_{LA \rightarrow N_I H}(s) = \frac{C_A}{8\pi} (Y_\nu^\dagger Y_\nu)_{II} g^2 \mathcal{F}_g \left(\frac{s}{m_{\text{th}}^2(T)} \right). \quad (\text{D22})$$

Detailed HTL-resummed expressions and precise values of \mathcal{F}_g for the individual gauge channels can be found in [54–56].

³ HTL masses are temperature-dependent effective masses that particles acquire from interactions in a hot plasma, computed

within the Hard Thermal Loop approximation [57].

Per-particle rates and comparison with Hubble rate for the top- and Gauge-assisted scatterings

For equilibration we require the *per-particle* rate, normalized to one heavy neutrino N_I :

$$\Gamma_{\text{scatt}}^{(\Delta L=1)}(T) \equiv \frac{\gamma_{\Delta L=1}(T)}{n_{N_I}^{\text{eq}}(T)}, \quad (\text{D23})$$

where $\gamma_{\Delta L=1}$ is the sum of the relevant $\Delta L = 1$ reaction densities involving N_I . In the relativistic limit ($T \gg M_I$), the equilibrium number density of a Majorana fermion ($g_N = 2$) is

$$n_{N_I}^{\text{eq}}(T) = \frac{3\zeta(3)}{2\pi^2} T^3. \quad (\text{D24})$$

For a slowly varying reduced cross section $\hat{\sigma}(s) \approx \hat{\sigma}_0$, Eq. (C4) gives

$$\gamma(T) \simeq \frac{\hat{\sigma}_0 T^4}{16\pi^4}, \quad (\text{D25})$$

using $\int_0^\infty dx x^2 K_1(x) = 2$. Thus

$$\Gamma_{\text{scatt}}(T) = \frac{\gamma(T)}{n_{N_I}^{\text{eq}}(T)} \simeq \frac{\hat{\sigma}_0}{24\zeta(3)\pi^2} T. \quad (\text{D26})$$

The scattering rate for top-assisted scatterings can be determined using Eq. (D16):

$$\Gamma_{\text{top},I}^{(\Delta L=1)}(T) \simeq \frac{3\bar{\mathcal{F}}_t}{192\zeta(3)\pi^3} (Y_\nu^\dagger Y_\nu)_{II} y_t^2 T \equiv c_t (Y_\nu^\dagger Y_\nu)_{II} y_t^2 T, \quad (\text{D27})$$

with $c_t = 3\bar{\mathcal{F}}_t/(192\zeta(3)\pi^3) \approx (2-4) \times 10^{-4}$, which parametrizes the theoretical uncertainties associated with thermal masses, IR regularization and phase-space approximations. Instead, for gauge-assisted processes and using Eq. (D22), we find

$$\Gamma_{\text{gauge},I}^{(\Delta L=1)}(T) \simeq \frac{C_A \bar{\mathcal{F}}_g}{192\zeta(3)\pi^3} (Y_\nu^\dagger Y_\nu)_{II} g^2 T \equiv c_g (Y_\nu^\dagger Y_\nu)_{II} g^2 T, \quad (\text{D28})$$

with $c_g = C_A \bar{\mathcal{F}}_g/(192\zeta(3)\pi^3) \approx (1-3) \times 10^{-4}$.

Summing the dominant channels,

$$\Gamma_{\text{scatt}}^{(\Delta L=1)}(T) \equiv \Gamma_{\text{top},I}^{(\Delta L=1)} + \Gamma_{\text{gauge},I}^{(\Delta L=1)} \simeq c_1 (Y_\nu^\dagger Y_\nu)_{II} (y_t^2 + g^2) T, \quad (\text{D29})$$

with an effective coefficient

$$c_1 \approx (3-7) \times 10^{-4}, \quad (\text{D30})$$

once thermal masses, angular dependence and channel multiplicities are taken into account, in agreement with detailed numerical studies [54–56]. The variation in the parameters c_t , c_g and consequently c_1 parametrizes the theoretical uncertainty from thermal masses, IR regularization and phase-space approximations in the $\Delta L = 1$ scatterings.

In the aligned limit $\Gamma_{\text{scatt}}^{(\Delta L=1)}(T)$ can be rewritten as

$$\Gamma_{\text{scatt}}^{(\Delta L=1)}(T) \simeq 2c_1 \frac{m_{\nu,I} M_I}{v_h^2} (y_t^2 + g^2) T. \quad (\text{D31})$$

Therefore, the ratio between the scattering and the Hubble rate is

$$\frac{\Gamma_{\text{scatt}}^{(\Delta L=1)}(T)}{H(T)} \simeq \frac{2c_1}{1.66\sqrt{g_*}} \frac{m_{\nu,I} M_{\text{Pl}}}{v_h^2} (y_t^2 + g^2) \frac{M_I}{T}. \quad (\text{D32})$$

For $m_{\nu,I} \sim 0.05$ eV, $g_* \sim 10^2$, $y_t^2 + g^2 = \mathcal{O}(1)$ and $c_1 \sim 5 \times 10^{-4}$ one obtains for $T \sim M_I$

$$\frac{\Gamma_{\text{scatt}}^{(\Delta L=1)}}{H} \gtrsim \mathcal{O}(1). \quad (\text{D33})$$

2. Portal processes involving R and χ

(a) $RR \leftrightarrow HH$. The cross section of the process $RR \leftrightarrow HH$ depends on κ_{loop} . In fact, for $T \gg m_H, m_R$ it scales as

$$\sigma(RR \rightarrow HH) \sim \frac{\kappa_{\text{loop}}^2}{16\pi s}, \quad s \sim T^2. \quad (\text{D34})$$

The per-particle rate is

$$\Gamma_{RR \rightarrow HH} \sim n_R^{\text{eq}} \sigma \sim \kappa_{\text{loop}}^2 T, \quad (\text{D35})$$

up to $\mathcal{O}(10^{-1})$ factors. For the values relevant in our model, $\kappa_{\text{loop}} \sim 10^{-11} - 10^{-10}$, hence $\Gamma_{RR \rightarrow HH}/T \sim 10^{-20}$ and $\Gamma_{RR \rightarrow HH} \ll H(T)$ at all temperatures of interest. Thus $RR \leftrightarrow HH$ is completely negligible for thermal contact.

(b) $N_I R \rightarrow LH$. The process $N_I R \rightarrow L_\alpha H$ proceeds through the combination of the Majorana coupling $R N_I N_I$ and the Dirac Yukawa $L_\alpha H N_I$. In the mass basis (and in the limit where R couples diagonally to N_I), the relevant interactions are

$$-\mathcal{L} \supset \frac{1}{2} y_{N,I} R \overline{N_I^c} N_I + y_{\alpha I} \overline{L_\alpha} \tilde{H} N_I + \text{h.c.}, \quad (\text{D36})$$

so that $N_I R \rightarrow L_\alpha H$ proceeds dominantly via s -channel N_I exchange. In the unbroken phase and for $T \gg m_{\text{EW}}$, taking all external masses (except M_I) negligible, the reduced cross section $\hat{\sigma}(s) \equiv 2s\sigma(s)$ is

$$\hat{\sigma}_{N_I R \rightarrow LH}(s) = \frac{1}{8\pi} |y_{N,I}|^2 (Y_\nu^\dagger Y_\nu)_{II} \mathcal{F}_{NR} \left(\frac{s}{M_I^2} \right), \quad (\text{D37})$$

where \mathcal{F}_{NR} is a dimensionless kinematic function that encodes the exact angular dependence and the mild s/M_I^2 dependence. For $s \gtrsim (2T)^2 \gg M_I^2$ one has

$$\mathcal{F}_{NR}(x) \xrightarrow{x \gg 1} 1 \quad \text{up to } \mathcal{O}\left(\frac{M_I^2}{s}\right) \text{ corrections.} \quad (\text{D38})$$

We therefore take an effective thermal average $\bar{\mathcal{F}}_{NR} \sim 0.5-2$ for $T \sim \text{few} \times M_I$.

Using Eq. (C4) the per-particle rate is

$$\Gamma_{N_I R \rightarrow LH}(T) \equiv \frac{\gamma_{N_I R \rightarrow LH}}{n_{N_I}^{\text{eq}}} \simeq \frac{\hat{\sigma}_0}{24\zeta(3)\pi^2} T = c_{NR} |y_{N,I}|^2 (Y_\nu^\dagger Y_\nu)_{II} T, \quad (\text{D39})$$

with

$$c_{NR} = \frac{\bar{\mathcal{F}}_{NR}}{192\zeta(3)\pi^3} \approx (0.7-2.8) \times 10^{-4}. \quad (\text{D40})$$

This is directly analogous to the c_t and c_g factors obtained for the top- and gauge-assisted $\Delta L = 1$ scatterings.

In the aligned Casas–Ibarra limit one finds

$$\Gamma_{N_I R \rightarrow LH}(T) \simeq 2 c_{NR} \frac{y_{N,I}^2 m_{\nu,I} M_I}{v_h^2} T. \quad (\text{D41})$$

For illustration, take $m_{\nu,I} = 0.05$ eV, $v_h = 246$ GeV, $g_* = 106.75$, and $c_{NR} \sim 10^{-4}$. Using Eq. (D41), the rate at $T \simeq M_I$ is

$$\frac{\Gamma_{N_I R \rightarrow LH}}{H} \simeq 0.12 \left(\frac{c_{NR}}{10^{-4}} \right) \left(\frac{y_{N,I}}{1} \right)^2 \left(\frac{m_{\nu,I}}{0.05 \text{ eV}} \right) \left(\frac{106.75}{g_*} \right)^{1/2}, \quad (\text{D42})$$

independent of M_I at $T = M_I$. Thus, for $y_{N,I} \sim 1$ this channel contributes at the level $\Gamma/H \sim 0.1$ near $T \simeq M_I$, while larger Yukawas $y_{N,I} \gtrsim 3$ would make it fully efficient ($\Gamma/H \gtrsim 1$). For fixed M_I , the ratio scales as $\Gamma/H \propto M_I/T$ at higher temperatures, decreasing slowly for $T \gg M_I$, analogously to the standard $\Delta L = 1$ scatterings.

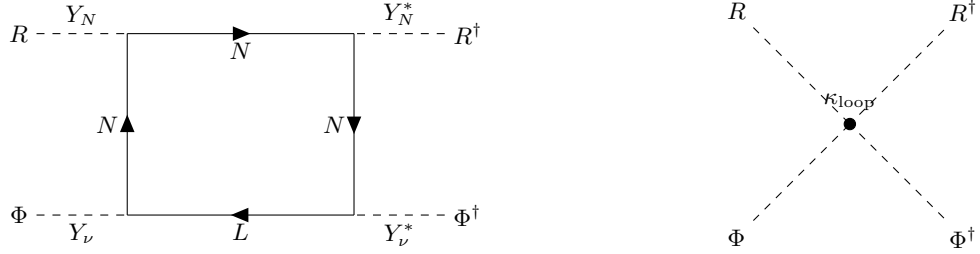


FIG. 5. One-loop generation of the mixed quartic $(\Phi^\dagger \Phi)(R^\dagger R)$. Left: box diagram with two Y_N and two Y_ν insertions and internal N, L lines. Right: effective contact interaction with coupling κ_{loop} obtained by integrating out the heavy neutrinos for $p^2 \ll M_N^2$.

a. Summary

Process hierarchy and temperature trends. For seesaw-motivated parameters ($m_{\nu,I} \sim 0.05$ eV, $y_{N,I} = \mathcal{O}(1)$, $M_I \gtrsim \text{few TeV}$, $g_* \simeq 10^2$):

- **Decays/inverse decays** $N_I \leftrightarrow LH$:

$$\frac{\langle \Gamma_{D,I} \rangle_T}{H} = \frac{m_{\nu,I} M_{\text{Pl}}}{4\pi 1.66 \sqrt{g_*} v_h^2} \xi^2 \frac{K_1(\xi)}{K_2(\xi)}.$$

For $\xi \ll 1$ (very high T), this scales as $\propto \xi^3$ and is small; as the Universe cools to $\xi \sim \mathcal{O}(1)$ ($T \sim M_I$) the ratio grows to $\mathcal{O}(10-30)$ and *dominates* equilibration.

- $\Delta L = 1$ scatterings (top- and gauge-assisted):

$$\frac{\Gamma_{\text{scatt}}^{(\Delta L=1)}}{H} \simeq \frac{2c_1}{1.66\sqrt{g_*}} \frac{m_{\nu,I} M_{\text{Pl}}}{v_h^2} (y_t^2 + g^2) \frac{M_I}{T} \propto \frac{M_I}{T}.$$

They are typically $\mathcal{O}(1)$ at $T \sim M_I$ and provide efficient additional channels; for $T \gg M_I$ the ratio decreases slowly as M_I/T .

- **Portal scattering** $N_I R \leftrightarrow L_\alpha H$: at $T = M_I$

$$\left. \frac{\Gamma_{N_I R \rightarrow LH}}{H} \right|_{T=M_I} \simeq 0.1-0.2 \left(\frac{c_{NR}}{10^{-4}} \right) \left(\frac{m_{\nu,I}}{0.05 \text{ eV}} \right) \left(\frac{y_{N,I}}{1} \right)^2, \quad (\text{D43})$$

where the numerical range reflects the mild dependence on g_* . For $y_{N,I} = \mathcal{O}(1)$ and $m_{\nu,I}$ in the experimentally favored range, the portal scattering is *subdominant* compared to decays and the standard $\Delta L = 1$ scatterings, but still non-negligible. For larger Yukawas $y_{N,I} \gtrsim 3$ it can become fully efficient ($\Gamma/H \gtrsim 1$), further assisting SM-dark-sector thermal contact.

- **Loop-induced scalar portal** $RR \leftrightarrow HH$: $\Gamma/H \ll 1$ throughout the parameter space of interest and can be safely neglected for thermal contact.

Overall: As the Universe cools down to $T \sim \text{few} \times M_I$, N_I decays/inverse decays become the *dominant* equilibration channel. $\Delta L = 1$ scatterings are efficient and comparable to decays around $T \sim M_I$, while $N_I R \leftrightarrow LH$ provides an additional but subleading portal for $y_{N,I} \sim 1$, becoming important only for larger $y_{N,I}$. At $T \ll M_I$ all N_I -mediated reactions decouple due to Boltzmann suppression of N_I .

Appendix E: Radiative generation of the mixed quartic $(\Phi^\dagger \Phi)(R^\dagger R)$

In this appendix we show how the mixed quartic $\kappa (\Phi^\dagger \Phi)(R^\dagger R)$ is generated at one loop from the neutrino Yukawa interactions if it is absent (or highly suppressed) at tree level. We focus on the part of the Lagrangian relevant for the loop, namely the Yukawa terms,

$$\mathcal{L} \supset -Y_\nu^{\alpha i} \overline{L_\alpha} \tilde{\Phi} N_i - \frac{1}{2} Y_N^{ij} R \overline{N_i^c} N_j + \text{h.c.}, \quad (\text{E1})$$

and assume that the tree-level portal $\kappa_0(\Phi^\dagger\Phi)(R^\dagger R)$ vanishes in the UV (e.g. due to an approximate symmetry or sequestering). The leading contribution to κ is then radiative, generated by the box diagram in the left panel of Fig. 5, which induces an effective $(\Phi^\dagger\Phi)(R^\dagger R)$ interaction once the heavy neutrinos are integrated out (right panel). For clarity, we first consider a single generation: one lepton doublet L , one Majorana fermion N with mass M_N , and couplings Y_ν and Y_N (the three-flavour case is given at the end).

The Feynman rule for the vertex RNN is $iY_N P_R - iY_N^* P_L$, while for ΦLN it is $-iY_\nu P_R$. We match the four-point function $\Phi R \rightarrow \Phi^\dagger R^\dagger$ at vanishing external momenta. In the regime $p_{\text{ext}}^2 \ll M_N^2$, the amplitude admits a local expansion and the leading term is the Wilson coefficient of $(\Phi^\dagger\Phi)(R^\dagger R)$. Higher orders in p_{ext}^2/M_N^2 map onto derivative operators and are irrelevant for κ . In our setup $M_{N_i} \gtrsim 10$ TeV, so for all phenomenological applications $p^2/M_{N_i}^2 \ll 1$ and the zero-momentum matching is an excellent approximation.

a. *Single generation: loop evaluation.* Choosing a fermion-flow orientation along the loop, the box gives

$$i\mathcal{M} = (-1)(-iY_N)(-iY_N^*)(-iY_\nu)(-iY_\nu^*) \int \frac{d^d k}{(2\pi)^d} \text{Tr}[P_R S_N(k) P_L S_N(k) P_L S_L(k) P_R S_N(k)], \quad (\text{E2})$$

where the overall minus sign is for the closed fermion loop. Inserting propagators,

$$i\mathcal{M} = -|Y_N|^2 |Y_\nu|^2 \int \frac{d^d k}{(2\pi)^d} \frac{\mathcal{N}(k)}{(k^2 - M_N^2)^3 k^2}, \quad (\text{E3})$$

with

$$\mathcal{N}(k) = \text{Tr}[P_R(k + M_N) P_L(k + M_N) P_L k P_R(k + M_N)] = 2M_N^2 k^2. \quad (\text{E4})$$

Thus

$$i\mathcal{M} = -|Y_N|^2 |Y_\nu|^2 2M_N^2 \int \frac{d^d k}{(2\pi)^d} \frac{1}{(k^2 - M_N^2)^3}. \quad (\text{E5})$$

In dimensional regularization ($d = 4 - 2\epsilon$),

$$I_3(M_N) \equiv \mu^{2\epsilon} \int \frac{d^d k}{(2\pi)^d} \frac{1}{(k^2 - M_N^2)^3} = \frac{i}{16\pi^2} \frac{1}{2M_N^2} \left[\frac{1}{\epsilon} - \gamma_E + \ln(4\pi) + \ln \frac{\mu^2}{M_N^2} + 1 \right], \quad (\text{E6})$$

whence

$$i\mathcal{M} = -i \frac{|Y_N|^2 |Y_\nu|^2}{16\pi^2} \left[\frac{1}{\epsilon} - \gamma_E + \ln(4\pi) + \ln \frac{\mu^2}{M_N^2} + 1 \right]. \quad (\text{E7})$$

The low-energy EFT contains $\mathcal{L}_{\text{EFT}} \supset -\kappa(\mu)(\Phi^\dagger\Phi)(R^\dagger R) \Rightarrow i\mathcal{M}_{\text{EFT}} = -i\kappa_{\text{loop}}(\mu)$. Matching in $\overline{\text{MS}}$ and subtracting $\frac{1}{\epsilon} - \gamma_E + \ln 4\pi$ yields

$$\kappa_{\text{loop}}(\mu) = \frac{|Y_N|^2 |Y_\nu|^2}{16\pi^2} \left[\ln \frac{M_N^2}{\mu^2} - 1 \right]. \quad (\text{E8})$$

Choosing $\mu \simeq M_N$ minimizes the logarithm and gives

$$\kappa_{\text{loop}}(M_N) = -\frac{|Y_\nu|^2 |Y_N|^2}{16\pi^2}. \quad (\text{E9})$$

Using the one-generation seesaw relation (aligned limit), $(Y_\nu^\dagger Y_\nu) = 2m_\nu M_N/v_h^2$, Eq. (E8) can be written as

$$\kappa_{\text{loop}}(\mu) = -\frac{y_N^2 M_N}{8\pi^2 v_h^2} m_\nu + \frac{m_\nu y_N^2 M_N}{8\pi^2 v_h^2} \ln \frac{M_N^2}{\mu^2}, \quad \Rightarrow \quad \kappa_{\text{loop}}(M_N) = -\frac{y_N^2 M_N}{8\pi^2 v_h^2} m_\nu. \quad (\text{E10})$$

Here y_N denotes the (real) eigenvalue of Y_N in the one-generation case. The sign of the loop-induced κ is scheme-dependent, but physical observables such as the mixing angle α and the scalar masses are RG- and scheme-independent; only these combinations have physical meaning.

b. *Three generations and the choice of μ .* For three generations and in the Casas–Ibarra aligned limit ($O = \mathbb{1}$) one has $(Y_\nu^\dagger Y_\nu)_{II} = 2m_{\nu,I} M_I / v_h^2$. Generalizing Eq. (E8) to three flavours and working in the heavy-neutrino mass basis gives

$$\kappa_{\text{loop}}(\mu) = - \sum_{I=1}^3 \frac{y_{N,I}^2 M_I}{8\pi^2 v_h^2} m_{\nu,I} + \sum_{I=1}^3 \frac{y_{N,I}^2 M_I}{8\pi^2 v_h^2} m_{\nu,I} \ln \frac{M_I^2}{\mu^2}, \quad \Rightarrow \quad \kappa_{\text{loop}}|_{\mu=M_I \text{ (stepwise)}} = - \sum_{I=1}^3 \frac{y_{N,I}^2 M_I}{8\pi^2 v_h^2} m_{\nu,I}. \quad (\text{E11})$$

With a *single* renormalization scale μ , one can cancel the logarithm for *at most one* heavy mass; it is not possible to choose $\mu = M_I$ for all loops simultaneously if the M_I are non-degenerate. Only if $M_1 \simeq M_2 \simeq M_3 \equiv M$ can a single choice $\mu = M$ make all logs small. The correct multi-scale treatment is stepwise EFT matching: integrate out each N_I at $\mu \simeq M_I$ (so its log vanishes and leaves the finite threshold -1), then run κ between thresholds.

Appendix F: Renormalization-Group Evolution of the Portal Coupling κ

In this appendix we clarify how the Higgs–singlet portal coupling κ evolves under renormalization-group (RG) running once the tree-level value $\kappa(\Lambda) = 0$ is imposed at the UV scale Λ , and why the loop-induced contribution generated at the heavy-neutrino threshold M_N remains extremely small at all lower energies.

We assume that the scalar portal

$$\kappa(\Lambda) (\Phi^\dagger \Phi)(R^\dagger R) \quad (\text{F1})$$

is absent at the UV scale Λ , due to sequestering, a symmetry, or a non-abelian UV origin of the dark gauge group [24, 38, 41–46]. Since in our model no light degrees of freedom carry simultaneously SM and dark charge, no tree-level operator can regenerate κ at lower scales. The leading nonzero contribution arises at the scale where the heavy neutrinos N_I are integrated out. As shown in Sec. E, the one-loop box diagram involving the neutrino Yukawas Y_ν and Y_N generates the effective quartic

$$\Delta\kappa \equiv \kappa_{\text{loop}} \simeq - \sum_{I=1}^3 \frac{y_{N,I}^2 M_{N,I}}{8\pi^2 v_h^2} m_{\nu,I}, \quad (\text{F2})$$

which is proportional to the light neutrino masses $m_{\nu,I}$. Numerically, for $m_{\nu,I} \sim 0.05$ eV, $y_{N,I} \sim 1$, and $M_{N,I} \sim \mathcal{O}(10)$ TeV, one finds $|\kappa_{\text{loop}}| \sim 10^{-13}\text{--}10^{-12}$, with only mild variations in the multi-TeV range. This value serves as the matching condition at $\mu \simeq M_N$.

Below the heavy-neutrino scale, the effective theory contains only Φ , R , χ , and SM fields. Crucially, after the heavy neutrinos are integrated out there are *no* light fields simultaneously charged under the SM and the dark sector that can source a new $(\Phi^\dagger \Phi)(R^\dagger R)$ operator. As a result, the beta function for κ has no additive term and takes the multiplicative form

$$\beta_\kappa(\mu) \equiv \frac{d\kappa}{d \ln \mu} = \kappa(\mu) \mathcal{F}(\lambda_H, \lambda_R, y_p, g_i, \dots), \quad (\text{F3})$$

where \mathcal{F} is a polynomial in the low-energy couplings. The solution is

$$\kappa(\mu) = \kappa(M_N) \exp \left[\int_\mu^{M_N} d \ln \mu' \mathcal{F}(\mu') \right]. \quad (\text{F4})$$

Thus the RG evolution of κ is purely multiplicative (logarithmic): the origin $\kappa = 0$ is an RG fixed point. In particular, if the portal vanishes at the matching scale,

$$\kappa(M_N) = 0 \quad \Rightarrow \quad \kappa(\mu) = 0 \quad \forall \mu < M_N, \quad (\text{F5})$$

and RG running cannot generate a nonzero tree-level portal at lower energies. Physically, this reflects the absence of particles carrying both SM and dark quantum numbers: once the heavy neutrinos are removed from the spectrum, no loop diagram can “reconnect” Φ with R unless the portal is already present.

If instead the portal is generated radiatively at the threshold, $\kappa(M_N) = \kappa_{\text{loop}} \neq 0$, then Eq. (F4) shows that $\kappa(\mu)$ simply undergoes multiplicative running,

$$\kappa(\mu) = \kappa_{\text{loop}} \exp \left[\int_\mu^{M_N} d \ln \mu' \mathcal{F}(\mu') \right]. \quad (\text{F6})$$

The exponent is controlled by SM quartics, Yukawas, and gauge couplings and is at most $\mathcal{O}(1)$ between the electroweak scale and M_N , leading to an overall variation by at most a factor of a few, $\kappa(\mu) \sim (1-10) \kappa_{\text{loop}}$. Therefore, in the neutrino-aligned scenario considered in this work, the portal coupling remains extremely small along the entire RG flow, with a typical upper size

$$\kappa(\mu) \lesssim \mathcal{O}(10^{-11}) \quad \text{for all } \mu < M_N, \quad (\text{F7})$$

unless one adds new messenger fields with sizeable SM and dark charges or abandons the seesaw-motivated parameter regime.

Appendix G: Decoupling and freeze-out with two temperatures ($T' \neq T$)

This appendix collects the ingredients used in the main text to describe the decoupling of the neutrino portal and the subsequent dark-sector freeze-out in the regime where the SM bath and the hidden sector evolve with different temperatures $T' \neq T$. We adopt the notation of App. D: M_I denotes the heavy-neutrino masses, $\zeta \equiv T'/T$ is the dark-to-visible temperature ratio, $g_*^{\text{vis}}(T)$ and $g_*^{\text{vis}}(T')$ are the usual visible-sector energy and entropy relativistic d.o.f., with analogous definitions for the dark sector.

1. Decoupling around $T \sim M_I$ and entropy bookkeeping

As the temperature drops below the mass of the lightest heavy neutrino $M_{N,I}$, the heavy-neutrino abundance becomes Boltzmann suppressed and portal-mediated energy exchange shuts off. From that moment on, the comoving entropies of the two sectors are separately conserved,

$$s_{\text{vis}}(T) a^3 = \text{const}, \quad s_{\text{dark}}(T', \{\mu_i(T')\}) a^3 = \text{const}, \quad (\text{G1})$$

where μ_i is the chemical potential for the particle species i . The temperature ratio at later times is fixed by separate entropy conservation after decoupling. Assuming full chemical equilibrium in the dark sector at the decoupling temperature T'_{dec} ($\mu_i(T'_{\text{dec}}) = 0$), the general expression is (see, e.g., [47])

$$\zeta(T) \equiv \frac{T'}{T} = \left[\frac{s_{\text{vis}}(T)}{s_{\text{vis}}(T_{\text{dec}})} \right]^{1/3} \left[\frac{s_{\text{dark}}(T'_{\text{dec}}, \{\mu_i=0\})}{s_{\text{dark}}(T' = \zeta T, \{\mu_i(T')\})} \right]^{1/3}. \quad (\text{G2})$$

If the following two physical conditions apply: (i) the relevant species in each sector behave as a radiation bath so that $s = \frac{2\pi^2}{45} g_* S T^3$, and (ii) *number-changing* reactions are fast enough to enforce $\mu_i = 0$, Eq. (G2) reduces to the familiar result (see e.g. [47])

$$\zeta(T) = \left[\frac{g_*^{\text{vis}}(T)}{g_*^{\text{vis}}(T_{\text{dec}})} \right]^{1/3} \left[\frac{g_*^{\text{dark}}(T'_{\text{dec}})}{g_*^{\text{dark}}(T')} \right]^{1/3}. \quad (\text{G3})$$

In typical benchmarks with $m_\chi \sim \mathcal{O}(\text{GeV})$ and $M_I \sim \mathcal{O}(\text{TeV})$, the ensuing ζ lies in the ballpark $\zeta \simeq 1-2$ (the precise value follows from the g_{*S} evolution in the two sectors).

2. Temperature ratio $\zeta \equiv T'/T$: general expression and benchmarks

In our minimal secluded setup the late-time dark bath is dominated by the real scalar H_p (mass m_{H_p}) and, depending on the benchmark, possibly by a light dark gauge boson Z' . The Dirac DM χ (mass m_χ) is Boltzmann suppressed at $T' \sim m_\chi/20$ and can be neglected in $g_{*S}^{\text{dark}}(T')$ unless explicitly stated.

In order to estimate the value of ζ at the epoch relevant for DM freeze-out, $T \simeq m_\chi/20$, we use the following inputs:

- Visible sector: $g_{*S}^{\text{vis}}(T_{\text{dec}}) = 106.75$, $g_{*S}^{\text{vis}}(T \simeq m_\chi/20) = 86.25$.
- Dark sector at decoupling: $g_{*S}^{\text{dark}}(T'_{\text{dec}}) = 4.5$ (Dirac χ + real scalar H_p). If a dark gauge boson Z' is relativistic at decoupling, use $g_{*S}^{\text{dark}}(T'_{\text{dec}}) = 7.5$.

TABLE I. Representative values of $\zeta \equiv T'/T$ at $T \simeq m_\chi/20$, obtained by solving Eq. (G3) self-consistently with $T' = \zeta T$, $g_{*S}^{\text{vis}}(T)/g_{*S}^{\text{vis}}(T_{\text{dec}}) = 86.25/106.75$, $g_{*S}^{\text{dark}}(T'_{\text{dec}}) = 4.5$ (Dirac χ + real scalar H_p), and exact scalar entropy for H_p (no light Z' at late times, $\mu_i = 0$).

m_{H_p} [GeV]	ζ for m_χ [GeV]				
	10	30	100	300	1000
1	1.296	1.238	1.236	1.236	1.236
3	1.601	1.296	1.238	1.236	1.236
10	1.872	1.639	1.296	1.238	1.236
30	1.894	1.872	1.601	1.296	1.238
100	1.895	1.894	1.872	1.639	1.236

- Chemical potentials: we assume efficient number-changing in the dark bath ($\mu_i = 0$) so that Eq. (G3) applies directly. After dark chemical freeze-out ($\mu_i > 0$) one must use the general form (G2), which typically yields a *smaller* ζ at fixed parameters.

Table I summarizes representative values of ζ as a function of m_{H_p} and m_χ in the minimal case (no light Z' at late times), assuming $\mu_i = 0$. The qualitative trends are: (i) for fixed m_χ , the heavier m_{H_p} , the larger ζ ; (ii) for fixed m_{H_p} , the larger m_χ , the smaller ζ . Across the broad range relevant here, ζ typically lies in the 1.1–1.9 band.

3. Dark freeze-out with $T' = \zeta T$

After visible–dark decoupling, the portal remains too feeble to re-equilibrate the sectors. The dark bath stays internally thermalized at temperature $T' = \zeta T$ through fast secluded reactions. For the Dirac dark matter particle χ (mass m_χ) annihilating into a lighter real scalar H_p ($m_{H_p} < m_\chi$) via the Yukawa interaction $y_p \bar{\chi} \chi H_p$, the dominant number-changing channel is

$$\chi \bar{\chi} \rightarrow H_p H_p. \quad (\text{G4})$$

We work with the visible–entropy yield $Y_\chi \equiv n_\chi/s_{\text{vis}}$, using $s_{\text{vis}}(T) = \frac{2\pi^2}{45} g_{*S}^{\text{vis}}(T) T^3$, and define

$$x \equiv \frac{m_\chi}{T}, \quad x' \equiv \frac{m_\chi}{T'} = \frac{x}{\zeta}. \quad (\text{G5})$$

During radiation domination, the Hubble rate receives contributions from the radiation in both sectors,

$$H(T) = \sqrt{\frac{8\pi G}{3} (\rho_{\text{vis}}(T) + \rho_{\text{dark}}(T'))} = \frac{\pi}{\sqrt{90}} \frac{T^2}{M_{\text{Pl}}} \left[g_{*}^{\text{vis}}(T) + g_{*}^{\text{dark}}(T') \zeta^4 \right]^{1/2} \equiv \frac{1.66 \sqrt{g_{*}^H(T, T')}}{M_{\text{Pl}}} T^2, \quad (\text{G6})$$

where

$$g_{*}^H(T, T') \equiv g_{*}^{\text{vis}}(T) + \zeta^4 g_{*}^{\text{dark}}(T') \quad (\text{G7})$$

is the energy degrees of freedom combination entering H .

The Boltzmann equation for Y_χ reads

$$\frac{dY_\chi}{dx} = -\frac{s_{\text{vis}}(T)}{x H(T)} \langle \sigma v \rangle_{\chi \bar{\chi} \rightarrow H_p H_p}(x') \left[Y_\chi^2 - (Y_\chi^{\text{eq}}(x'))^2 \right], \quad (\text{G8})$$

with $Y_\chi^{\text{eq}}(x') = n_\chi^{\text{eq}}(T')/s_{\text{vis}}(T)$ and where the annihilation rate must be evaluated at the *dark* temperature T' .

In App. A 4b we report the full calculation of the thermal average for the process $\chi \bar{\chi} \rightarrow H_p H_p$ that dominates the relic density:

$$\langle \sigma v \rangle_{\chi \bar{\chi} \rightarrow H_p H_p}(x') = \frac{6 b(r)}{x'} = \frac{y_p^4}{64\pi m_\chi^2} \mathcal{S}_p(r) \frac{6}{x'}. \quad (\text{G9})$$

For a Majorana χ the result is multiplied by 1/2 due to identical initial states. The kinematic limits are $\mathcal{S}_p(0) = 1$ (light mediator) and $\mathcal{S}_p(r) \propto (1-r)^{1/2}$ near threshold ($r \rightarrow 1$).

The freeze-out condition equates the *dark* annihilation rate to the *visible* Hubble rate,

$$n_\chi^{\text{eq}}(T') \langle \sigma v \rangle(T') \simeq H(T), \quad (\text{G10})$$

with $n_\chi^{\text{eq}}(T') \simeq g_\chi \left(\frac{m_\chi T'}{2\pi} \right)^{3/2} e^{-x'}$ in the non-relativistic regime. Using Eq. (G9) one obtains the standard logarithmic solution

$$x'_f \simeq \ln \left(\mathcal{A} y_p^4 \right) - \frac{1}{2} \ln \left[\ln \left(\mathcal{A} y_p^4 \right) \right], \quad (\text{G11})$$

with

$$\mathcal{A} \equiv \frac{c_f g_\chi m_\chi M_{\text{Pl}}}{1.66 (2\pi)^{3/2}} \frac{\zeta^2}{\sqrt{g_*^H(T_f, T'_f)}} \frac{6 \mathcal{S}_p(r)}{64\pi m_\chi^2}, \quad T_f \equiv \frac{m_\chi}{x_f}, \quad T'_f \equiv \frac{m_\chi}{x'_f}. \quad (\text{G12})$$

Here $c_f = \mathcal{O}(1)$ encodes the usual matching convention. For $m_\chi \sim \text{GeV}$ and $y_p \sim 0.1\text{--}1$ one finds $x'_f \in [20, 30]$, as in the standard p -wave freeze-out.

The solution of Eq. (G8) can be written in terms of the annihilation integral in the two-temperature case,

$$J_{2T} \equiv \int_{x_f}^{\infty} \frac{\langle \sigma v \rangle(x')}{x^2} dx = \frac{1}{\zeta} \left[\frac{a}{x'_f} + \frac{3b}{x'^2_f} \right]. \quad (\text{G13})$$

Using for the annihilation cross section Eq. (G9) (pure p -wave, $a = 0$) we find

$$J_{2T} = \frac{1}{\zeta} \frac{3 y_p^4}{64\pi m_\chi^2} \frac{\mathcal{S}_p(r)}{x'^2_f}. \quad (\text{G14})$$

Defining

$$\lambda_{\text{eff}} \equiv 0.264 \frac{g_{*S}^{\text{vis}}(T_f)}{\sqrt{g_*^H(T_f, T'_f)}} M_{\text{Pl}} m_\chi, \quad (\text{G15})$$

the asymptotic yield and relic density are

$$Y_\infty = \frac{1}{\lambda_{\text{eff}} J_{2T}}, \quad \Omega_\chi h^2 \simeq \left(1.05 \times 10^9 \text{ GeV}^{-1} \right) \frac{\sqrt{g_*^H(T_f, T'_f)}}{g_{*S}^{\text{vis}}(T_f)} \frac{1}{M_{\text{Pl}}} \frac{1}{J_{2T}}. \quad (\text{G16})$$

Specializing to p -wave only and inserting Eq. (G14),

$$\Omega_\chi h^2 \simeq \left(1.05 \times 10^9 \text{ GeV}^{-1} \right) \frac{\sqrt{g_*^H(T_f, T'_f)}}{g_{*S}^{\text{vis}}(T_f)} \frac{\zeta x'^2_f}{M_{\text{Pl}}} \frac{64\pi m_\chi^2}{3 y_p^4 \mathcal{S}_p(r)}. \quad (\text{G17})$$

Inverting Eq. (G17) for the coupling,

$$y_p = \left[\left(1.05 \times 10^9 \text{ GeV}^{-1} \right) \frac{\sqrt{g_*^H(T_f, T'_f)}}{g_{*S}^{\text{vis}}(T_f)} \frac{\zeta x'^2_f}{M_{\text{Pl}}} \frac{64\pi m_\chi^2}{3 \Omega_\chi h^2 \mathcal{S}_p(r)} \right]^{1/4}. \quad (\text{G18})$$

A useful numerical estimate is

$$y_p \simeq 0.43 \left(\frac{x'_f}{25} \right)^{1/2} \left(\frac{m_\chi}{100 \text{ GeV}} \right)^{1/2} \left(\frac{g_{*S}^{\text{vis}}}{86.25} \right)^{-1/4} \left(\frac{g_*^H}{100} \right)^{1/8}. \quad (\text{G19})$$

Therefore, a value of $y_p \sim \mathcal{O}(0.1\text{--}1)$ is needed to reach the observed DM relic density. We show in Fig. 6 the values of y_p for which DM achieves the observed relic density. Equivalently, a handy heuristic for the *required* thermal rate is

$$\langle \sigma v \rangle_{\text{req}} \approx \frac{2 \times 10^{-26} \text{ cm}^3 \text{ s}^{-1}}{\zeta} \left[1 + \mathcal{O} \left(\frac{g_*^{\text{dark}}}{g_*^{\text{vis}}} \zeta^4 \right) \right], \quad (\text{G20})$$

i.e. a hotter (colder) dark bath with $\zeta > 1$ ($\zeta < 1$) requires a *smaller* (*larger*) annihilation cross section to reproduce the observed $\Omega_{\text{DM}} h^2$.

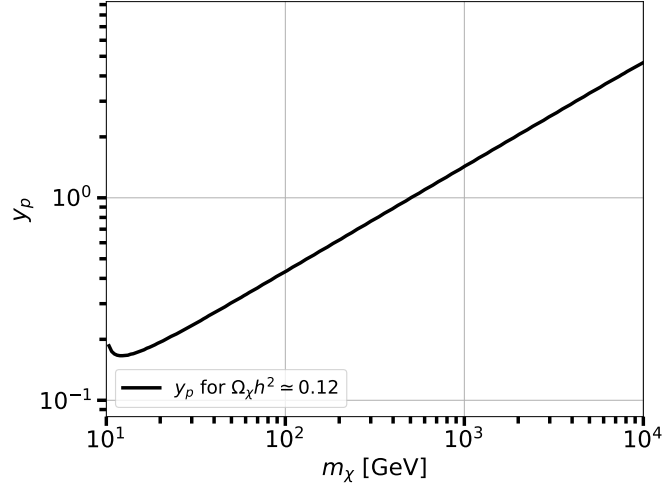


FIG. 6. Values of y_p for which DM achieves the observed relic density.

Appendix H: Spin-independent nuclear cross section

Spin-independent scattering of the DM particle χ off a nucleon $N = p, n$ proceeds via t -channel exchange of the CP-even scalars H and H_p . In our model the relevant couplings are

$$g_{\chi\chi H} = \frac{y_p}{\sqrt{2}} \sin \alpha, \quad g_{\chi\chi H_p} = \frac{y_p}{\sqrt{2}} \cos \alpha, \quad g_{HNN} = \frac{m_N}{v_h} f_N \cos \alpha, \quad g_{H_p NN} = -\frac{m_N}{v_h} f_N \sin \alpha, \quad (\text{H1})$$

where $f_N \simeq 0.30$ is the nucleon scalar form factor, defined through the matrix element

$$m_N f_N = \sum_{q=u,d,s} \langle N | m_q \bar{q}q | N \rangle. \quad (\text{H2})$$

The spin-independent cross section on a nucleon is

$$\sigma_{\chi N}^{\text{SI}} = \frac{\mu_N^2}{\pi} \left[\sum_{i=H,H_p} \frac{g_{\chi\chi h_i} g_{h_i NN}}{m_{h_i}^2} \right]^2 = \frac{\mu_N^2 m_N^2 f_N^2 y_p^2}{2\pi v_h^2} \sin^2 \alpha \cos^2 \alpha \left(\frac{1}{m_H^2} - \frac{1}{m_{H_p}^2} \right)^2, \quad (\text{H3})$$

with μ_N the χ - N reduced mass. This expression exhibits a ‘‘blind spot’’ when $m_H \simeq m_{H_p}$, where the two scalar contributions nearly cancel. In what follows we focus instead on the *small-mixing* regime relevant for secluded DM, $\sin \alpha \ll 1$.

For small mixing angles, the H - H_p mixing is controlled by the mixed quartic κ in the potential $V(\Phi, R) \supset \kappa(\Phi^\dagger \Phi)(R^\dagger R)$, where κ is connected to the mixing angle through

$$\tan 2\alpha = \frac{2\kappa v_h v_r}{m_{H_p}^2 - m_H^2}. \quad (\text{H4})$$

In the small-mixing limit ($|\alpha| \ll 1$),

$$\sin \alpha \cos \alpha = \frac{1}{2} \sin 2\alpha \simeq \frac{1}{2} \tan 2\alpha \simeq \frac{\kappa v_h v_r}{m_{H_p}^2 - m_H^2}. \quad (\text{H5})$$

Inserting Eq. (H5) into Eq. (H3), one finds the compact form

$$\sigma_{\chi N}^{\text{SI}} = \frac{\mu_N^2 m_N^2 f_N^2 y_p^2}{2\pi} \frac{\kappa^2 v_r^2}{m_H^4 m_{H_p}^4}. \quad (\text{H6})$$

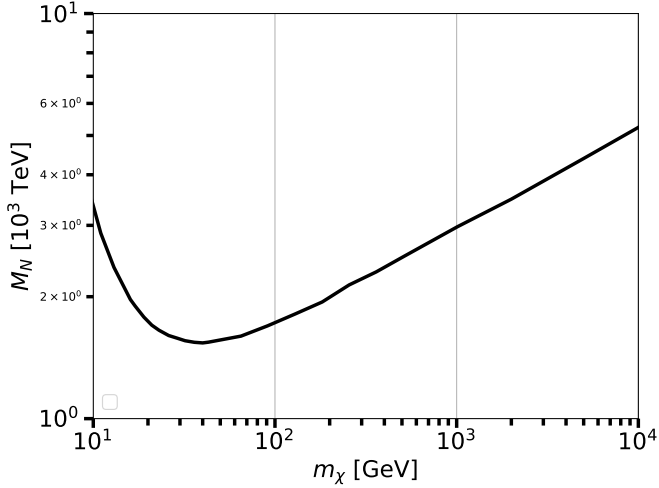


FIG. 7. Upper limit on the heavy-neutrino mass M_N as a function of the DM mass m_χ , obtained by applying the spin-independent limits from Ref. [17] to our model (see Eq. H9).

The portal coupling κ is generated radiatively by the neutrino sector if it vanishes (or is highly suppressed) at tree level. In the Casas–Ibarra aligned limit ($O = \mathbb{1}$) and for three generations the loop-induced portal coupling is (see Eq. E11)

$$\kappa_{\text{loop}}(\mu) = - \sum_{I=1}^3 \frac{y_{N,I}^2 M_I}{8\pi^2 v_h^2} m_{\nu,I}. \quad (\text{H7})$$

Inserting Eq. (H7) into Eq. (H6) and *eliminating* v_r in favour of M_N and y_N , one finds

$$\sigma_{\chi N}^{\text{SI}} = \frac{\mu_N^2 m_N^2 f_N^2 y_p^2}{64\pi^5 m_H^4 m_{H_p}^4 v_h^4} \left(\sum_{I=1}^3 y_{N,I}^2 m_{\nu,I}^2 M_I^4 \right). \quad (\text{H8})$$

This form has *no* residual dependence on v_r : the cross section is fully expressed in terms of y_N , M_N , the light neutrino masses $m_{\nu,I}$, and known SM parameters. A numerical form of Eq. (H8) is

$$\sigma_{\chi N}^{\text{SI}} \simeq 3.9 \times 10^{-57} \text{ cm}^2 \left(\frac{m_\chi}{m_\chi + m_N} \right)^2 \left(\frac{y_p}{1} \right)^2 \left(\frac{10 \text{ GeV}}{m_{H_p}} \right)^4 \sum_{I=1}^3 \left(\frac{y_{N,I}}{1} \right)^2 \left(\frac{m_{\nu,I}}{0.05 \text{ eV}} \right)^2 \left(\frac{M_{N,I}}{10 \text{ TeV}} \right)^4. \quad (\text{H9})$$

Just to provide a rough estimate of the bounds on the model from the latest LZ spin-independent limit, we can take $m_\chi \simeq 100$ GeV, for which $\sigma_{\text{LZ}} \simeq 3.5 \times 10^{-48} \text{ cm}^2$. Using the single-generation version of Eq. (H9) (with $m_{H_p} = 10$ GeV) and solving for M_N , one finds an upper limit for the heavy-neutrino mass of the order of

$$M_N \lesssim 1.7 \times 10^3 \text{ TeV} \left(\frac{1}{y_p y_N} \right)^{1/2} \left(\frac{0.05 \text{ eV}}{m_\nu} \right)^{1/2} \left(\frac{m_{H_p}}{10 \text{ GeV}} \right). \quad (\text{H10})$$

For $y_p \sim 1$ (the value required to reach the correct relic abundance, see Eq. G19), $y_N \sim 1$, $m_\nu \sim 0.05$ eV and $m_{H_p} \sim 10$ GeV, the loop-induced scalar portal is safely consistent with LZ bounds for heavy-neutrino masses up to the few- 10^3 TeV scale. In Fig. 7 we show the upper limits for M_N obtained when changing m_χ . We can see that the upper limits remain in the few PeV range even changing the DM mass. In other words, within this radiative portal setup, current direct-detection limits do not impose a strong upper bound on M_N ; the requirement $|\tan \alpha| \lesssim 10^{-3}$ is easily satisfied throughout the parameter space of interest.

[1] J. Silk *et al.*, *Particle Dark Matter: Observations, Models and Searches*, edited by G. Bertone (Cambridge Univ. Press, Cambridge, 2010).

[2] G. Bertone and D. Hooper, *Rev. Mod. Phys.* **90**, 045002 (2018), arXiv:1605.04909 [astro-ph.CO].

[3] M. Cirelli, A. Strumia, and J. Zupan, (2024), arXiv:2406.01705 [hep-ph].

[4] G. Bertone, D. Hooper, and J. Silk, *Phys. Rept.* **405**, 279 (2005), arXiv:hep-ph/0404175.

[5] B. W. Lee and S. Weinberg, *Phys. Rev. Lett.* **39**, 165 (1977).

[6] J. E. Gunn, B. W. Lee, I. Lerche, D. N. Schramm, and G. Steigman, *Astrophys. J.* **223**, 1015 (1978).

[7] J. Wess and B. Zumino, *Nuclear Physics B* **70**, 39 (1974).

[8] H. Goldberg, *Phys. Rev. Lett.* **50**, 1419 (1983).

[9] J. R. Ellis, J. S. Hagelin, D. V. Nanopoulos, K. A. Olive, and M. Srednicki, *Nucl. Phys. B* **238**, 453 (1984).

[10] G. Steigman and M. S. Turner, *Nucl. Phys. B* **253**, 375 (1985).

[11] M. Schumann, *J. Phys. G* **46**, 103003 (2019), arXiv:1903.03026 [hep-ex].

[12] A. Boveia and C. Doglioni, *Ann. Rev. Nucl. Part. Sci.* **68**, 429 (2018), arXiv:1810.12238 [hep-ex].

[13] J. M. Gaskins, *Contemp. Phys.* **57**, 496 (2016), arXiv:1604.00014 [astro-ph.HE].

[14] N. Aghanim *et al.* (Planck), (2018), arXiv:1807.06209 [astro-ph.CO].

[15] J. Aalbers *et al.*, *Phys. Rev. Lett.* **131**, 041002 (2023), arXiv:2207.03764 [hep-ex].

[16] E. Aprile *et al.*, *Phys. Rev. Lett.* **131**, 041003 (2023).

[17] J. Aalbers *et al.* (LZ), *Phys. Rev. Lett.* **135**, 011802 (2025), arXiv:2410.17036 [hep-ex].

[18] G. Arcadi, M. Dutra, P. Ghosh, M. Lindner, Y. Mambrini, M. Pierre, S. Profumo, and F. S. Queiroz, *Eur. Phys. J. C* **78**, 203 (2018), arXiv:1703.07364 [hep-ph].

[19] G. Arcadi, A. Djouadi, and M. Raidal, *Phys. Rept.* **842**, 1 (2020), arXiv:1903.03616 [hep-ph].

[20] M. Di Mauro, C. Arina, N. Fornengo, J. Heisig, and D. Massaro, *Phys. Rev. D* **108**, 095008 (2023), arXiv:2305.11937 [hep-ph].

[21] G. Arcadi, D. Cabo-Almeida, M. Dutra, P. Ghosh, M. Lindner, Y. Mambrini, J. P. Neto, M. Pierre, S. Profumo, and F. S. Queiroz, (2024), arXiv:2403.15860 [hep-ph].

[22] M. Di Mauro and B. Xie, (2025), arXiv:2510.08677 [hep-ph].

[23] M. Pospelov, A. Ritz, and M. B. Voloshin, *Phys. Lett. B* **662**, 53 (2008), arXiv:0711.4866 [hep-ph].

[24] M. Pospelov and A. Ritz, *Phys. Lett. B* **671**, 391 (2009), arXiv:0810.1502 [hep-ph].

[25] M. Di Mauro and Y. Wang, (2025), arXiv:2510.23771 [hep-ph].

[26] N. Aghanim *et al.*, *Astron. Astrophys.* **641**, A6 (2020), arXiv:1807.06209 [astro-ph.CO].

[27] A. G. Adame *et al.* (DESI Collaboration), (2024), neutrino-mass constraints within Λ CDM; see text for caveats in extended models, arXiv:2404.03002 [astro-ph.CO].

[28] I. Esteban, M. C. Gonzalez-Garcia, M. Maltoni, I. Martinez-Soler, J. P. Pinheiro, and T. Schwetz, *JHEP* **12**, 216, arXiv:2410.05380 [hep-ph].

[29] M. Aker *et al.* (KATRIN), *Science* **388**, adq9592 (2025), arXiv:2406.13516 [nucl-ex].

[30] P. Minkowski, *Phys. Lett. B* **67**, 421 (1977).

[31] T. Yanagida, in *Proceedings of the Workshop on the Unified Theory and the Baryon Number in the Universe* (1979).

[32] M. Gell-Mann, P. Ramond, and R. Slansky, *Conf. Proc. C* **790927**, 315 (1979).

[33] R. N. Mohapatra and G. Senjanovic, *Phys. Rev. Lett.* **44**, 912 (1980).

[34] D. Wyler and L. Wolfenstein, *Nucl. Phys. B* **218**, 205 (1983).

[35] R. N. Mohapatra and J. W. F. Valle, *Phys. Rev. D* **34**, 1642 (1986).

[36] S. Baek, P. Ko, and W.-I. Park, *JHEP* **02**, 047, arXiv:1112.1847 [hep-ph].

[37] S. Baek, P. Ko, and W.-I. Park, *JHEP* **07**, 013, arXiv:1303.4280 [hep-ph].

[38] B. Holdom, *Phys. Lett. B* **166**, 196 (1986).

[39] R. Essig *et al.*, (2013), arXiv:1311.0029 [hep-ph].

[40] J. A. Casas and A. Ibarra, *Nucl. Phys. B* **618**, 171 (2001), arXiv:hep-ph/0103065.

[41] K. R. Dienes, C. F. Kolda, and J. March-Russell, *Nucl. Phys. B* **492**, 104 (1997), hep-ph/9610479.

[42] N. Arkani-Hamed, S. Dimopoulos, and G. R. Dvali, *Phys. Lett. B* **429**, 263 (1998), hep-ph/9803315.

[43] L. Randall and R. Sundrum, *Phys. Rev. Lett.* **83**, 3370 (1999), hep-ph/9905221.

[44] M. A. Luty and R. Sundrum, *Phys. Rev. D* **65**, 066004 (2002), hep-th/0105137.

[45] L. Randall and R. Sundrum, *Nucl. Phys. B* **557**, 79 (1999), hep-th/9810155.

[46] D. Feldman, B. Kors, and P. Nath, *Phys. Rev. D* **75**, 023503 (2007), 0707.1873.

[47] T. Bringmann, P. F. Depta, M. Hufnagel, and K. Schmidt-Hoberg, *Phys. Lett. B* **817**, 136341 (2021), arXiv:2007.03696 [hep-ph].

[48] M. Fukugita and T. Yanagida, *Phys. Lett. B* **174**, 45 (1986).

[49] W. Buchmuller, P. Di Bari, and M. Plumacher, *Annals Phys.* **315**, 305 (2005), arXiv:hep-ph/0401240 [hep-ph].

[50] S. Davidson, E. Nardi, and Y. Nir, *Phys. Rept.* **466**, 105 (2008), arXiv:0802.2962 [hep-ph].

[51] S. F. King, *Rept. Prog. Phys.* **67**, 107 (2004), arXiv:hep-ph/0310204 [hep-ph].

[52] J. Heeck, *Phys. Rev. D* **86**, 093023 (2012), arXiv:1207.5521 [hep-ph].

[53] I. Cordero-Carrión, M. Hirsch, and A. Vicente, *Phys. Rev. D* **101**, 075032 (2020), arXiv:1912.08858 [hep-ph].

[54] G. F. Giudice, A. Notari, M. Raidal, A. Riotto, and A. Strumia, *Nucl. Phys. B* **685**, 89 (2004), arXiv:hep-ph/0310123.

[55] C. S. Fong, E. Nardi, and A. Riotto, *Adv. High Energy Phys.* **2012**, 158303 (2012), arXiv:1301.3062 [hep-ph].

[56] F. Hahn-Woernle, M. Plumacher, and Y. Y. Y. Wong, *JCAP* **09**, 010, arXiv:0907.0205 [hep-ph].

[57] E. Braaten and R. D. Pisarski, *Nucl. Phys. B* **339**, 310 (1990).